RM L53A09

NACA RM L53A09

NACA

RESEARCH MEMORANDUM

LANGLEY FULL-SCALE-TUNNEL TESTS OF THE

CUSTER CHANNEL WING AIRPLANE

By Jerome Pasamanick

Langley Aeronautical Laboratory
Langley Field, Va.

NATIONAL ADVISORY COMMITTEE
FOR AERONAUTICS

WASHINGTON

April 7, 1953

NATIONAL ADVISORY COMMITTEE FOR AERONAUTICS

RESEARCH MEMORANDUM

LANGLEY FULL-SCALE-TUNNEL TESTS OF THE CUSTER CHANNEL WING AIRPLANE

By Jerome Pasamanick

SUMMARY

As a part of a research program to study the principles involved in the use of propeller slipstreams and jets to increase lift, an experimental Custer Channel Wing airplane has been tested in the Langley full-scale tunnel to investigate the lift characteristics of a channel-propeller combination and the flow phenomena in and about a channel wing. Some of the general stability and control characteristics of the airplane were also studied at tunnel airspeeds from approximately 25 to 40 mph. Emphasis was placed on determining the airplane static lift characteristics (zero airspeed) for the basic configuration and for several modifications. The effect of a ground boundary on the airplane static characteristics was investigated by testing the airplane both on the ground and out of the influence of the ground. Photographs of the tuft surveys made to determine the air-flow distribution around the channel and tail surfaces are included.

The significant findings of the static tests are summarized briefly as follows:

(a) The channel-propeller configuration in the static condition without ground effect produced a resultant force inclined 23° upward from the propeller thrust axis.

(b) The magnitude of the static resultant force with the propellers operating at about 2,450 rpm (170 horsepower total for both propellers) was approximately 88 percent of the static thrust calculated for these propellers when not in the presence of the channels.

(c) The airplane, having a normal tail configuration, had neither trim nor control effectiveness at zero forward speeds.

INTRODUCTION

There is renewed interest in airplanes capable of hovering and flying at very low airspeeds, as well as attaining satisfactory performance at cruising and high speeds. In this connection the NACA has started a basic research program to study the principles involved in the use of propeller slipstreams and blowing jets to increase lift. As a part of this program the NACA has undertaken tests of a full-scale experimental Custer Channel Wing airplane to study the static and low-speed lift-producing capabilities of the channel-wing principle as well as to study some of the stability and control characteristics of the experimental airplane at zero airspeed and low forward speeds at high angles of attack.

The primary objective of this investigation was to determine the amount of lift that would be produced by the operation of propellers located at the rear of open wing channels of semicircular cross section to induce a flow of air through the channels. The magnitude and direction of the corresponding resultant force were determined for various power conditions at zero airspeed. Also a brief investigation was made of the static stability and control characteristics of the experimental airplane at zero airspeed and at tunnel airspeeds of about 26 to 41 mph over an angle-of-attack range of -2° to 46°. A few of these tests were conducted with the airplane yawed 5° and 10°. The static tests were conducted with the airplane mounted in the tunnel (tunnel inoperative) in the absence of ground effect and also with the airplane on the ground in a three-point attitude to investigate ground effect. The test conditions of propeller operation, blade angle, and propeller-channel configuration were carefully controlled to satisfy the conditions prescribed by the designer for the experimental flight configuration.

SYMBOLS

The data are presented with respect to the stability axes which constitute an orthogonal system of axes having the origin at the airplane center of gravity, the Z-axis in the plane of symmetry and perpendicular to the relative wind in the forward-flight tests or vertical in the static tests, the X-axis in the plane of symmetry and perpendicular to the Z-axis, and the Y-axis perpendicular to the plane of symmetry. The positive directions of the forces and moments measured about these axes are shown in figure 1. The center-of-gravity location is shown in figure 2.

The data are presented in coefficient form for airspeeds of 26 mph or greater. It is emphasized that the forces and moments created by propeller operation at these low airspeeds produce large coefficients because of the low dynamic pressure. This is particularly true of the lift coefficient at high angles of attack because the propellers operating at high

thrust produce a force component in the lift direction in addition to the wing lift and therefore produce lift coefficients that are very large at low airspeeds and that are infinite when the airplane is at rest. For this reason, actual forces and moments rather than coefficients are used in presenting the data from the static tests or tests at airspeeds of 11.5 mph or lower. For the static tests where there is no wind, the vertical component of the resultant force is called the lift and the horizontal component along the X-axis is called the longitudinal force, positive when directed forward with respect to the airplane.

C_L lift coefficient, $\frac{\text{Lift}}{q \times \text{Wing area}}$, where lift is the component of the resultant force perpendicular to the relative wind and the wing area is the projected area of the channel wings S_c, unless specified otherwise

C_X longitudinal-force coefficient, $\frac{\text{Longitudinal force}}{qS_c}$, where longitudinal force is the component of the resultant force along the X-axis, positive upstream (When the airplane is at zero yaw (or sideslip), $C_X = -C_D$ where C_D is the drag coefficient $\frac{\text{Drag}}{qS_c}$. C_X is positive when the thrust component along the X-axis exceeds the drag component.)

C_Y lateral-force coefficient, $\frac{\text{Lateral force}}{qS_c}$, where lateral force is the force along the Y-axis, positive to the right

C_m pitching-moment coefficient, M/qS_cc

C_l rolling-moment coefficient, L/qS_cb

C_n yawing-moment coefficient, N/qS_cb

D drag, lb

M pitching moment about Y-axis, positive when nose is raised, ft-lb

L rolling moment about X-axis, positive when right wing is depressed, ft-lb

N yawing moment about Z-axis, positive when right wing is retarded, ft-lb

R	resultant force, $\sqrt{(\text{Lift})^2 + (\text{Longitudinal force})^2}$, lb
q	free-stream dynamic pressure, $\frac{1}{2}\rho V^2$, lb/sq ft
q_{av}	average free-stream dynamic pressure during an angle-of-attack run, $\frac{1}{2}\rho V_{av}^2$, lb/sq ft
ρ	mass density of air, slugs/cu ft
V	free-stream velocity, ft/sec unless specified otherwise
V_{av}	average free-stream velocity during an angle-of-attack run, ft/sec unless specified otherwise
S_c	projected area of channel wings, 35 sq ft
S_t	total area including the ailerons and the projected fuselage area intercepted by the channels, 59 sq ft
c	channel chord, measured in a plane parallel to plane of symmetry, 35 in.
b	airplane span, 20.25 ft
δ_e	elevator control deflection, measured perpendicular to hinge line, positive when trailing edge is down, deg
δ_r	rudder control deflection, measured perpendicular to hinge line, positive when trailing edge is left, deg
α	angle of attack of channel-wing-chord line (which is parallel to the thrust axis) referred to relative air stream in forward-flight tests and to the horizontal in static tests, deg
β	angle of sideslip, positive when left wing is retarded, deg
θ	inclination of resultant force, $\tan^{-1}\frac{\text{Lift}}{\text{Longitudinal force}}$, deg
HP	total horsepower input to motors

MODEL AND TESTS

The Custer Channel Wing airplane supplied by the Custer Channel Wing Corporation was an experimental airplane in which Continental C-90 internal-combustion engines of approximately 90 horsepower driving 6-foot-diameter metal propellers were mounted in two wing channels attached to a light-plane airframe. The airplane as received with an uncovered fuselage framework weighed approximately 900 pounds empty. The tail arrangement of this configuration was a conventional airplane-tail installation.

For the tests reported herein, the airplane fuselage was covered with fabric and the internal-combustion engines were replaced by variable-speed electric motors because the original internal-combustion engines were not adequately lubricated for operation at very high angles of attack. The use of electric motors also permitted approximate measurements of the power input. A drawing of the Custer Channel Wing airplane as tested is presented as figure 2 and photographs showing the airplane mounted in the tunnel and on the ground setup are given as figure 3.

The power input to the motors was determined from current-torque calibrations of the individual electric motors and also checked by the conventional determination of power by means of wattmeters. It is noted here that the propeller-operating wind-tunnel and ground tests were conducted under different motor control conditions. In the tunnel both motors were operated at the same speed because only a single source of variable-frequency supply and control was available, which resulted in a maximum propeller speed of 2,450 rpm as dictated by the particular motor drawing its maximum rated current. When the port motor was operated alone, however, it was possible to attain a speed of 2,645 rpm before reaching its limiting current rating. For the ground tests, on the other hand, an additional power source was made available and it was possible by special manipulation of the control equipment to run each motor independently and even at overload conditions to attain 2,625 rpm, producing 220-horsepower total output for both motors as compared to about 170 horsepower at 2,450 rpm.

In the course of the tests in the tunnel a power difference of the order of 15 to 20 horsepower existed between the two motors. Inasmuch as both the right-hand (starboard) and left-hand (port) propellers were carefully set at 11.5° blade angle at the 0.75-radius station, the power asymmetry can be accounted for by a dissymmetry in either the geometry of the two propellers or the channels, or perhaps both. Except for some thrust dissymmetry which introduced lateral and directional trim shifts, the power dissymmetry does not reflect a primary influence on the significance of the lift results of this investigation.

The elevator and rudder control surfaces were remotely controlled by electric actuators and the control-surface deflections were recorded from calibrated control-position transmitters. The horizontal tail had a fixed 10° nose-down incidence with respect to the channel-chord plane and the ailerons were locked in a neutral position with respect to the channel-chord plane.

Propeller-removed tests were conducted over the low airspeed range. The propeller speed, blade angle, and axial location, with respect to the trailing edge of the channel wing, were selected and carefully controlled to agree with conditions formerly used by the manufacturer in level-flight tests. Most of the tests were made with the center of the propeller tip chord 3/4 inch inside the channel-wing trailing edge (propeller tip trailing edge at the channel trailing edge) and with a minimum of blade tip clearance (approximately 1/16 inch). Some tests were conducted with the center of the propeller tip chord at the channel-wing trailing edge and for these runs the blade tip clearance was no more than 3/8 inch. In the latter part of the wind-tunnel test program, several runs were made with an extensible leading-edge flap and an extended trailing-edge flap installed on each channel, as shown in figure 2. It should be noted that the deflection angle, chord, and camber of the extensible leading-edge flaps are not necessarily optimum configurations for a simulated shroud contour but should at least approximate the effect of a more generous leading-edge radius.

The airplane was tested over a range of angle of attack and airspeed from about 2 to 41 mph in the wind tunnel at zero sideslip with propellers operating, and several tests were made at approximately -5° and -10° angles of sideslip for small negative and high positive angles of attack. The elevator and rudder control effectiveness was obtained for the forward-flight conditions at several angles of attack.

Static tests (zero airspeed) were made both in the wind tunnel where the airplane was tested high enough above the tunnel ground board not to be influenced by ground effect for most test conditions and also on the hangar floor in a three-point attitude. The static tests in the absence of ground effect were conducted with the tunnel entrance nozzle blocked off with a tarpaulin in order to insure essentially zero tunnel airspeed (the airplane slipstreams would otherwise create an appreciable circulation in the tunnel). Long hanging tufts indicated undisturbed air ahead of and below the channels, which effectively represented a zero-velocity free-air condition. The ground tests of the airplane were conducted in the Langley full-scale-tunnel hangar with the entire door system opened to eliminate interference on the propeller slipstream. This location enabled the airplane to be located in an area free from natural wind. The airplane was mounted about 2 inches from the ground on a floating frame suspended from Baldwin SR-4 load cells which measured the lift and the longitudinal force at the desired test conditions. The attitude of

this arrangement simulated the three-point attitude ($\alpha \approx 19^\circ$) of the airplane resting on the ground.

In addition to the tests with both propellers operating or removed, some tests were made to determine the effect of both propellers windmilling at an average airspeed of approximately 26 mph as well as the effect of asymmetric power at about the same forward speed and at static conditions in the absence of a ground boundary. Some questions arose as to whether the airplane channel-flow characteristics might have been affected by replacing the engines with the smaller electric motors. Accordingly, a few additional ground tests were made with a nacelle, roughly representing the engine, built around the electric motors. (See fig. 4.) The modifications reduced the open frontal area of the channel to a value slightly less than that with the original internal-combustion engines.

CORRECTIONS AND RESULTS

The wind-tunnel forward-flight data have been corrected for jet-boundary and stream alinement effects. The tunnel blocking and support interference were sufficiently small that corrections were not applied. The corrected wind-tunnel forward-flight data are determined as follows:

$$\alpha^\circ_{corr} = \alpha^\circ_{tun} - 0.248C_L - 0.5^\circ$$

$$C_{L_{corr}} = C_L - 0.0087C_X$$

$$C_{X_{corr}} = C_X + 0.0087C_L + 0.0043C_L^2 - 0.0012$$

The figures showing the basic data are presented in the following order: The effects of propeller rotational speed, angle of attack, and control-surface deflection on the force and stall characteristics of the airplane in static or near-static conditions as determined in the absence of ground effect are presented in figures 5 to 8. Figures 9, 10, and 11 show the effect of the horizontal tail on the static force and flow characteristics of the airplane with and without the modified nacelle in the presence of a ground boundary. The basic aerodynamic characteristics at low forward velocities are given in figures 12 and 13 for the propellers inoperative and operative, respectively. Results of tuft observation studies of the flow behavior at low forward velocities are shown in figure 14. The effects of control-surface deflection on the model characteristics for low-speed conditions are presented in figures 15, 16, and 17 for the rated, windmilling, and asymmetric power conditions, respectively. The airplane characteristics in sideslip are given in figure 18 and the effects of the presence of the ailerons on the airplane longitudinal characteristics are given in figure 19.

DISCUSSION OF RESULTS

Longitudinal Characteristics

Static tests in the absence of ground effect.- The static lift, longitudinal force, and pitching moment of the airplane as obtained in the wind tunnel for the propeller located with the center of its tip-chord trailing edge 3/4 inch inside the trailing edge of the channel wing and operating at 2,450 rpm were 340 pounds, 800 pounds, and -350 foot-pounds, nose down, respectively, at $\alpha = 0^\circ$ (fig. 5(a)). The corresponding resultant force and inclination of the resultant-force vector with respect to α were 880 pounds and 23° (fig. 7). The nose-down pitching moment would require a tail force in the negative lift direction for trim in hovering which would further reduce the magnitude and inclination of the resultant-force vector. Thus, provided a suitable tail could be obtained for the airplane to provide the negative tail force, the airplane, in order to hover, would have to be inclined at some angle greater than 67° and the weight would have to be less in magnitude than the resultant force.

There is a small reduction in the magnitude of the resultant force with angle of attack which would not be expected if power were constant and if the slipstream and flow about the channels experienced free-air conditions. Although there is a small power decrease, it is reasoned that the decrease in the lift force, which at $\alpha = 46^\circ$ is about 40 pounds, is caused by a certain amount of ground effect on the flow about the airplane in the tunnel when the airplane is at very high angles of attack. (See fig. 3(a).)

The results presented in figure 8 show practically a constant pitching moment for all elevator deflections (zero elevator effectiveness) which indicates that the propeller slipstream passed completely below the tail and, therefore, the measured airplane static lift and longitudinal-force characteristics in the absence of ground effect were dependent only upon the wing and propeller characteristics. It should be noted in figure 8(c) that the pitching-moment curve indicates that there was some flow in the neighborhood of the tail at 46°. Reference to figure 3 again shows that for this high angle the tunnel ground board was probably not far enough below the tail to provide completely free-stream conditions. A visual tuft survey in the region behind the propeller plane at zero angle of attack showed that the propeller slipstream for the static flight condition was deflected well downward and underneath the tail. These results show that in the hovering or very low speed flight conditions, a problem exists with regard to obtaining longitudinal and directional control.

As mentioned previously, there was a power dissymmetry that occurred in these tests which, in the static condition at $\alpha = 0^{\circ}$ and at 2,450 rpm, caused rolling moments and yawing moments corresponding roughly to 50 pounds more lift and about 35 pounds more thrust on the starboard side than on the port side of the airplane (fig. 8). No basic significance is attached to this particular condition of test since, in flight, the pilot would be expected to control the thrust adequately by variable propeller pitch or by throttle adjustments.

Exploratory studies made early in the test program indicate that the selected locations of the propeller in the channel did not affect the static lift characteristics of the airplane (fig. 5(a)). The channel and propeller-blade deformations that occurred at the maximum propeller rotational speed (2,450 rpm) actually resulted in zero tip clearance over a small portion of the channel for each of the two propeller locations described previously. At 2,000 rpm, however, the data show approximately 20 pounds higher lift for the more forward propeller location having the nominal tip clearance of 1/16 inch. Visual flow studies, figure 6, indicate that shortly ahead of the propeller plane the flow along the bottom of the channel was steady but a region of stalled flow occurred along the sides of the channel. It was evident from the behavior of the tufts forward on the channel that leading-edge separation extended along the bottom of the channel and along the outboard side of the channel (downward rotation of the propeller). The fuselage fillet provided a more gradual inflow into the channel and eliminated the leading-edge stall along the inboard side of the channel. The channel leading-edge stall for this static condition is attributed to the high inflow angle in spite of the fairly favorable leading-edge radius and camber of the airfoil (NACA 4412). Inasmuch as an effective control of inflow into a fully shrouded propeller has been found to require a much more generous leading-edge radius than that used on this channel, an attempt was made to determine how much relief of the leading-edge stall would be possible by the addition of an extensible leading-edge flap. The results presented in figure 5(b) show that this particular application of an extensible leading-edge flap did not favorably affect the airplane characteristics, but the addition of an extended trailing-edge flap increased the lift by about 25 pounds, which would be expected from a more downward deflection of the slipstream. Any such attempt to increase the static lifting capabilities of the channel wing, either by a change in airfoil section to one having larger leading-edge radius and camber or by an external flap-type device, might not be compatible with good performance at the higher-speed forward-flight condition.

Effect of low airspeed.- The effects of a small forward wind velocity on the airplane characteristics at zero angle of sideslip with only the port motor operating are shown in figure 5(c). It can be seen from this figure that a wind velocity of 3 mph increases the lift by 20 pounds at 2,450 rpm and a velocity of 4 mph increases the lift by 30 pounds at

2,625 rpm. The increased lift resulted, in part, from the stabilization of the flow over the wing leading edge and into the channel. An example of the effects of a forward wind velocity on the lift and thrust capabilities of the airplane at several angles of attack with both propellers operating at 2,450 rpm is shown in the following table:

V, mph	$\alpha = 0^\circ$		$\alpha = 20^\circ$		$\alpha = 46^\circ$	
	Lift, lb	Longitudinal force, lb	Lift, lb	Longitudinal force, lb	Lift, lb	Longitudinal force, lb
0	340	800	580	635	770	350
4	360	795	650	600	840	280
11.5	385	745	735	540	980	190
26	470	590	940	395	1375	-210

At the normal three-point attitude of the airplane ($\alpha \approx 20^\circ$) wind velocities of 4 mph and 11.5 mph increased the airplane total lift by 70 and 155 pounds, respectively, over that obtained in the static condition. It is considered that the improved leading-edge flow and more uniform flow into the propeller disk are at least partly responsible for this increased lift.

It is necessary to state that these tabulated lift results are for out-of-trim conditions and therefore can only be considered in approximate relationship. The lift requirement of the horizontal tail for trim would tend to decrease somewhat the total lift values shown at zero forward speed and to increase somewhat the total lift at a forward speed of 26 mph.

Static tests in presence of ground effect.- The lift characteristics of the airplane in the presence of the ground were appreciably influenced by the horizontal tail. (See fig. 9.) The data show that, with the tail off on the ground-test arrangement, the same lift and horizontal forces were obtained as with the tail on in the tunnel tests, which verifies that the wing flow and propeller flow are relatively unaffected by the presence of the ground and agrees with the previously mentioned observation that, in the tunnel tests at zero airspeed, the slipstream was below the tail. At the ground angle of 19° and a propeller speed of 2,450 rpm the total lift of the channel wing and vertical component of the propeller thrust (with $\delta_e = 0^\circ$) is about 690 pounds. Increasing the propeller rotational speed results in forces proportional to the square of the speed and horsepower proportional to the cube of the speed, which thereby verifies that no appreciable extraneous winds were present. Deflecting the elevator control down 20° resulted in an additional increase in lift of about 100 pounds. The removal of the horizontal tail reduced the lift of the airplane 104 and 135 pounds for the propeller operating at 2,450 and 2,625 rpm, respectively. The measured power input for the propeller

rotational speeds of 2,450 and 2,625 rpm were approximately 170 and 220 horsepower, respectively.

In order to visualize the air flow in the vicinity of the channel and to help explain the effectiveness of the tail in ground effect, the photographs presented in figure 10 show the flow pattern at various locations of the ground-test arrangement, and the following sketch illustrates the general flow pattern into the plane of the propeller. These flow characteristics were also present for the wind-tunnel arrangement where, however, it was not possible to survey the flow as completely as was done in the ground tests.

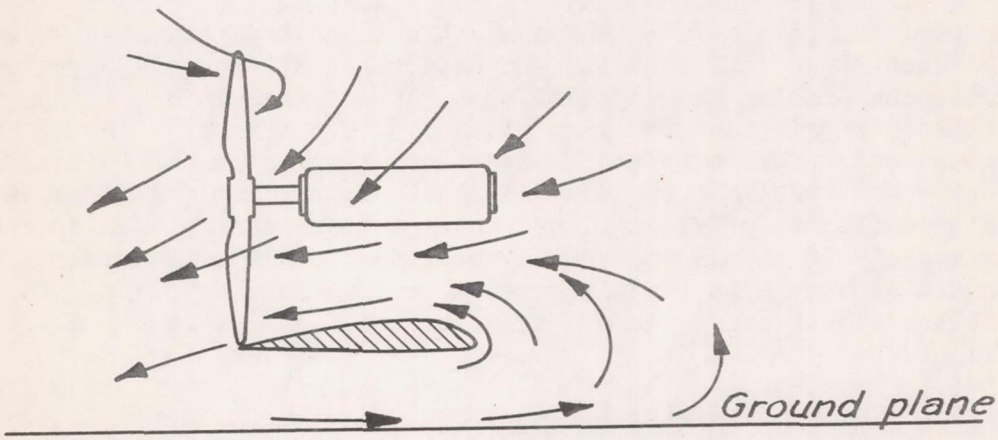

The air flow over the channel leading edge and extending approximately 2 inches above the channel surface is quite rough.

In the region ahead of and above the propeller hub axis and especially near the top of the propeller plane (fig. 10(a)), the inflow angle into the disk is very high (estimated to be about 75°). In fact, at the top of the propeller disk (fig. 10(b)) the air is seen to flow into the propeller from the downstream face. Inasmuch as the propeller is operating in nonuniform flow, its loading is asymmetrical and its efficiency, correspondingly, is lowered. A few preliminary surveys of the propeller slipstream immediately behind the plane of rotation indicated that the upper half, on the average, exhibited about one-half the dynamic-pressure rise of the lower half. It appeared that the outer 50-percent radius of the propeller in the lower 120° sector was the most effective portion of the propeller. The flow asymmetry observed is probably the major cause for the large difference between the measured longitudinal force of about 400 pounds per propeller and the calculated thrust of about 500 pounds for the same blade angle and tip speed. The acute downward deflection of the propeller slipstream directly behind and on the center line of the propeller plane and the large positive angle of upwash

in the region of the horizontal stabilizer can also be seen from the photographs in figure 10. It was evident that the horizontal tail was at a positive angle of attack in a flow field of fairly high dynamic pressure. The lift of the horizontal tail (fig. 9) was measured to be 15 percent and 25 percent of the total airplane lift with the elevator neutral and set at 20° (trailing edge down), respectively, for a propeller rotational speed of 2,450 rpm.

As was previously stated, the horizontal tail on the experimental airplane tested did not contribute at all to the airplane static lift when tested in the absence of ground effect in the wind tunnel. A concise comparison of the results with and without ground effect can be determined from table I. The ground effects on the present configuration are of such major importance that considerable study would have to be given to the problem and especially to the controls in attempting to design such an airplane for vertical ascent at take-off. In the absence of ground effect the airplane tested has a large nose-down pitching moment (about -350 foot-pounds) and, in order to trim the airplane longitudinally, the tail would be required to produce a down force of approximately 30 pounds, so that a net reduction of lift results. Accordingly, the large lift increments observed on the ground are of no particular significance since a negative tail lift is required for trim in flight.

Effect of nacelle installation.- The electric-motor—nacelle installation used in the present investigation resulted in a greater open-channel frontal area (measured in a plane parallel to the plane of rotation) than that for the internal-combustion-engine installation of the experimental flight airplane. In order to determine the effects of channel blockage on the propeller and channel static characteristics, a modified nacelle installation was tested on the ground-test arrangement. The frontal area blocked by the modified engine-nacelle mock-up was approximately two and one-half times the frontal area blocked by the electric-motor—nacelle installation used in the wind tunnel (see fig. 4) and was slightly greater than the blockage by the internal-combustion engines installed originally. The results at 2,450 rpm (figs. 9 and 11) show that the modified nacelles reduced the airplane lift by 40 pounds and also reduced the airplane longitudinal force by about 40 pounds.

Forward Flight

Characteristics with propellers removed.- The maximum lift coefficient (fig. 12) of the Custer Channel Wing airplane in the basic condition, propellers removed, was 2.2 and 2.1 for tunnel velocities of approximately 26 and 40 mph, respectively. Actually, in any one run, the tunnel dynamic pressures varied from about 2.2 pounds per square foot at $\alpha = 0^\circ$ to 1.5 pounds per square foot at the highest angle of attack for the low-airspeed data. For the higher-airspeed data, the tunnel dynamic

pressures varied from 4.4 to 3.9 pounds per square foot from the lowest to the highest angle of attack. The small decrease in $C_{L_{max}}$ (0.1) at the higher forward airspeed is considered to be the result of some increased roughness at the channel leading edge caused by the previous installation and removal of the flap (the data for 40 mph were obtained after the tests with the extensible leading-edge flaps were made). The results (fig. 12) indicate that, with regard to C_l, there was probably some asymmetry near and beyond the stall, resulting in the irregularity of the C_l curve, and that most of this asymmetry appears to have disappeared at the higher speed. The airplane had stable nose-down pitching moments at the stall for both airspeeds, but there is an unstable pitching tendency in the low C_L range.

It should be emphasized at this point that in the reduction of data the coefficients are based on the channel-wing area alone instead of the total area which is the normal procedure. Such a presentation, however, does not afford a direct comparison with other airplane configurations since the forward-speed results are influenced by the ailerons and the fuselage. In order to illustrate the point, the lift results in figures 12 and 13 are plotted also in coefficient form based on the total effective wing area, which include the ailerons and the projected fuselage area intercepted by the channels. It will be seen that the maximum values of C_L are comparable with those normally attained by conventional airplanes with thick wings and without high-lift devices.

Characteristics with propellers operating.- Varying the longitudinal location of the propeller plane in the channel had no significant effect on the lift characteristics of the airplane in forward flight, as was also found to be the case in static conditions. The rearward-located propeller in the forward-flight condition, however, decreased the longitudinal-force coefficients by approximately 0.3 and produced an unstable pitching-moment shift throughout the lift range (fig. 13(a)). Unless otherwise noted, the data of the following discussion were obtained with the rearward-located propeller in the channel.

With the propellers operating at 2,450 rpm, increasing the forward velocity resulted in more linear aerodynamic characteristics throughout the angle-of-attack range (fig. 13). Propeller operation contributed a destabilizing longitudinal-trim shift but apparently the stall remains stable. The irregularities in lateral force and yawing moments, which occurred at the lower speed ($\alpha \approx 24^\circ$, fig. 13(a)), were completely eliminated at the higher speed (fig. 13(b)). The large variations of the airplane lateral characteristics at the lower speed result from asymmetrical flow separation in the region just ahead of the propeller. The tuft surveys of figure 14 show the flow to be rough at the channel trailing edge for several degrees below the stall, followed by a complete and instantaneous flow breakdown on the lower part of the channel at $\alpha = 25.2^\circ$. It is of interest to note from figure 14 that the tufts indicated the direction

of flow on the channel surface to be inclined toward the lower part of the channel. This drainage of the flow from the side surfaces delayed the separation on these surfaces until higher angles of attack were reached. The forward-flight surveys of figure 14 (up to $\alpha \approx 25^{\circ}$) show the elimination of the leading-edge flow separation which occurred in the static flight condition (fig. 6).

A comparison of the lift-coefficient curves of figures 12 and 13 shows about a sevenfold increase in the values of the coefficient at a given angle of attack when power is applied which results primarily from the lift produced by the component of the propeller thrust in the lift direction. The rather large values of the lift coefficient are not of fundamental significance since the dynamic pressures for the low-velocity conditions are very low and ultimately the lift coefficients reach infinite values as the static condition is approached. It should be clearly defined that high values of lift coefficient are not unique for this particular configuration but would occur for any aircraft which approaches the hovering-flight condition.

It is emphasized that the large variation in the static longitudinal stability over the angle-of-attack range for the two forward-speed conditions shown in figure 13 signifies a serious problem of control in flight at the very low airspeeds. The untrimmed pitching moments (shown for neutral elevator) are large and, as shown later, cannot be trimmed with full control deflection. Some more effective tail configuration suitably located with respect to the existing flow field would have to be provided for these low airspeeds.

Miscellaneous stability and control measurements.- Although it was shown by the flow studies of the slipstream in the static-thrust investigation that the tail on this particular arrangement would not be in the slipstream and, therefore, could not trim or control the airplane in very low speed flight, it was still of some interest to obtain a little additional information on the effect of asymmetric power, power failure, higher forward velocity, and yaw on the elevator and rudder control effectiveness at a representative high angle of attack at a velocity of about 25 mph. The angle of attack was arbitrarily chosen to be in the vicinity where the component of the thrust along the X-axis equaled the drag component $\left(C_X \approx 0\right)$.

In general, these results show a very low control effectiveness for the windmilling propeller condition which is increased somewhat by propeller operation. The increased dynamic pressure at the tail is also accompanied, however, by an increased downwash and the configuration could not be trimmed in pitch for this power condition at the high angle of attack. Also, for the asymmetric thrust condition that prevailed in the forward-flight tests (about 25 pounds at $\alpha = 31^{\circ}$), full rudder deflection was required for directional trim. For single-engine operation, which would markedly increase the thrust asymmetry, the aerodynamic

controls would, therefore, be completely inadequate and flight would not be possible with single-engine operation.

The objective of this investigation did not include a study of the over-all performance at low or high speeds, inasmuch as the test configuration was not a prototype and embodied several compromises which produced high drag. Since single-engine flight provokes such serious problems that power-off landings would be required in event of failure of one engine, it is of interest to note that the maximum power-off lift-drag ratio for the configuration tested is very low (about 1.7), although this test configuration could undoubtedly be redesigned to give lower fuselage and engine installation drag. Nevertheless, the power-off landing would be a difficult maneuver with the small wing area of the experimental airplane tested if the landing speed were not sufficiently high to permit a flare, since for a given wing span a considerable amount of the channel surface contributes more drag than lift, and also since an engine nacelle supported by struts in a channel wing would be expected to have greater over-all drag than a conventional nacelle-wing configuration.

SUMMARY OF RESULTS

The results of the investigation in the Langley full-scale tunnel to determine the characteristics of an experimental Custer Channel Wing airplane at static conditions and over the low airspeed range are summarized as follows:

1. The resultant force and the pitching moment at static conditions (zero airspeed) in the absence of ground effect for the propeller operating at 2,450 rpm (170 horsepower total for both motors) were 880 pounds and about -350 foot-pounds, nose down, respectively. The resultant force was about 88 percent of the static thrust which the propellers were calculated to develop in the absence of the channels and was inclined 23° upward from the propeller thrust axis. Thus, provided a tail configuration could be obtained to trim the airplane, thereby reducing the magnitude and inclination of the resultant force, the airplane, to hover in the absence of ground effect, would have to be inclined at an angle greater than 67° and the weight would have to be less in magnitude than the resultant force.

2. There was no appreciable ground effect on the propeller-channel characteristics for the static condition.

3. The controls were completely inadequate under static lift conditions and the airplane could not be flown in hovering flight.

4. With the airplane resting on the ground there was an upward flow at the tail which increased the total lift about 200 pounds for the static condition. This lift force, however, is not significant since it would be completely eliminated for longitudinal trim as soon as the airplane tended to become airborne.

5. Small longitudinal displacement of the propeller plane did not appreciably affect the airplane static lift characteristics. Leading-edge stall occurred in the static flight condition and the single attempt to eliminate the stall by an extensible leading-edge flap did not measurably improve the airplane static lift characteristics. Small wind velocities did stabilize the flow over the leading edge and increased somewhat the lifting capabilities of the configuration.

6. Flow studies in the region of the propeller plane indicated high inflow angles into the upper unshrouded portion of the propeller with reversed flow occurring at the top of the propeller disk. The lower segment of the propeller disk was the more heavily loaded.

7. Low forward velocities greatly improved the flow into the channel wing and increasing the tunnel airspeed from about 25 mph to 40 mph resulted in more linear aerodynamic characteristics throughout the angle-of-attack range.

8. The airplane control effectiveness was low but essentially linear with control deflection in forward flight, so in the event of power failure the reduced control effectiveness caused by the loss of the propeller slipstream is an important design factor to consider. The asymmetric power condition also reduced the control effectiveness, and of considerable significance is the fact that the configuration would be uncontrollable with more than a small amount of power asymmetry resulting in a thrust dissymmetry of the order of 25 pounds at an airspeed of 25 mph.

Langley Aeronautical Laboratory,
National Advisory Committee for Aeronautics,
Langley Field, Va.

TABLE I

SUMMARY OF THE STATIC CHARACTERISTICS OF THE CUSTER CHANNEL WING AIRPLANE

Propeller speed, rpm	Control deflection, δ_e, deg	Tests with ground effect, $\alpha = 19^\circ$								Tests in the absence of ground effect, $\alpha = 20^\circ$			
		Tail on				Tail off				Tail on			
		Lift, lb	Longitudinal force, lb	R, lb	θ, deg	Lift, lb	Longitudinal force, lb	R, lb	θ, deg	Lift, lb	Longitudinal force, lb	R, lb	θ, deg
2450	0	688	698	980	44.6	584	677	893	40.7	581	635	861	42.5
	Down 20	786	641	1015	50.8	-	-	-	-	581	635	861	42.5
	Up 20	608	659	878	42.7	-	-	-	-	581	635	861	42.5
2625	0	788	762	1096	46.0	653	763	1005	40.6	-	-	-	-
	Down 20	904	731	1162	51.0	-	-	-	-	-	-	-	-
	Up 20	697	753	1027	42.8	-	-	-	-	-	-	-	-

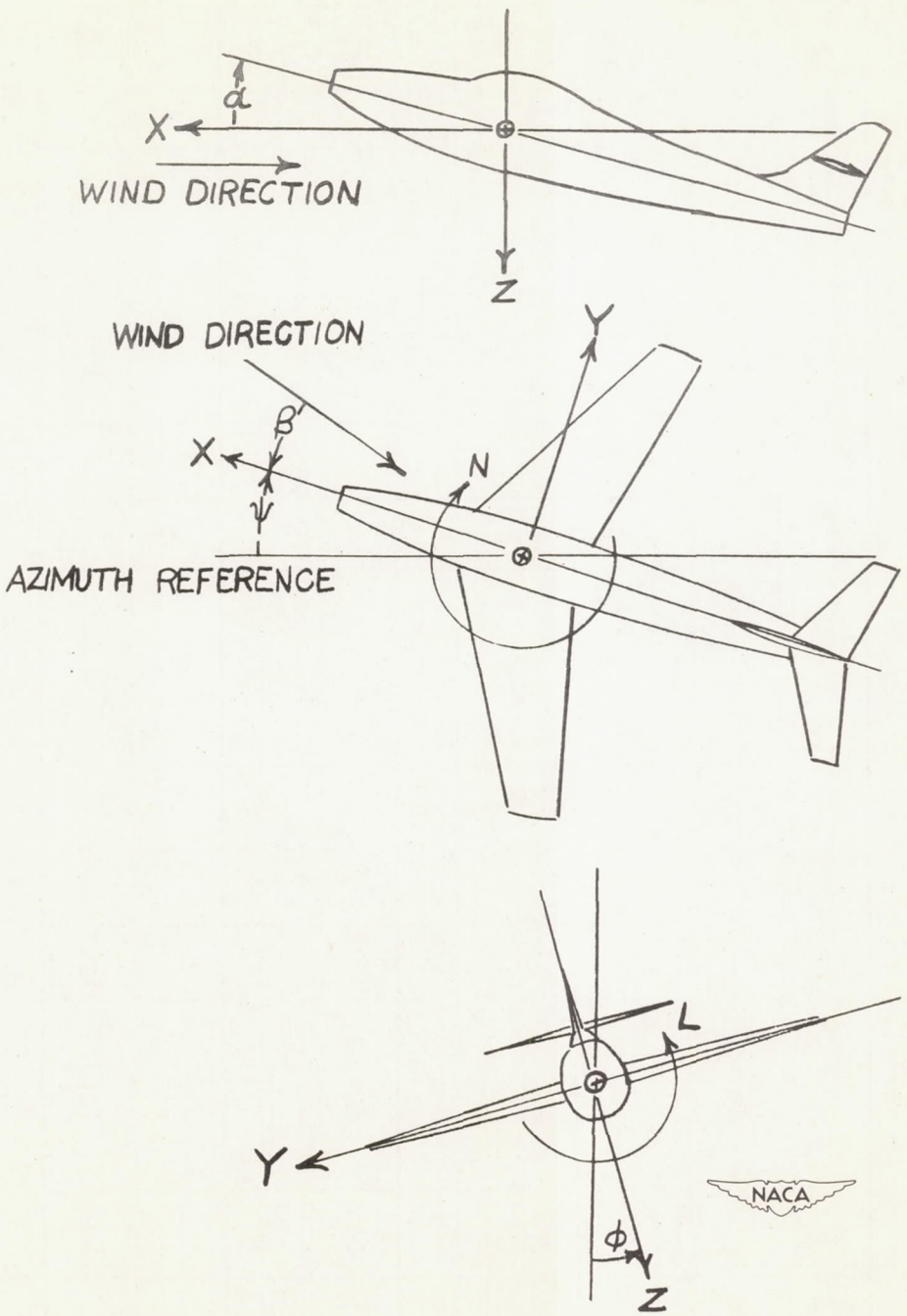

Figure 1.- The stability system of axes. Arrows indicate positive directions of moments, forces, and angles.

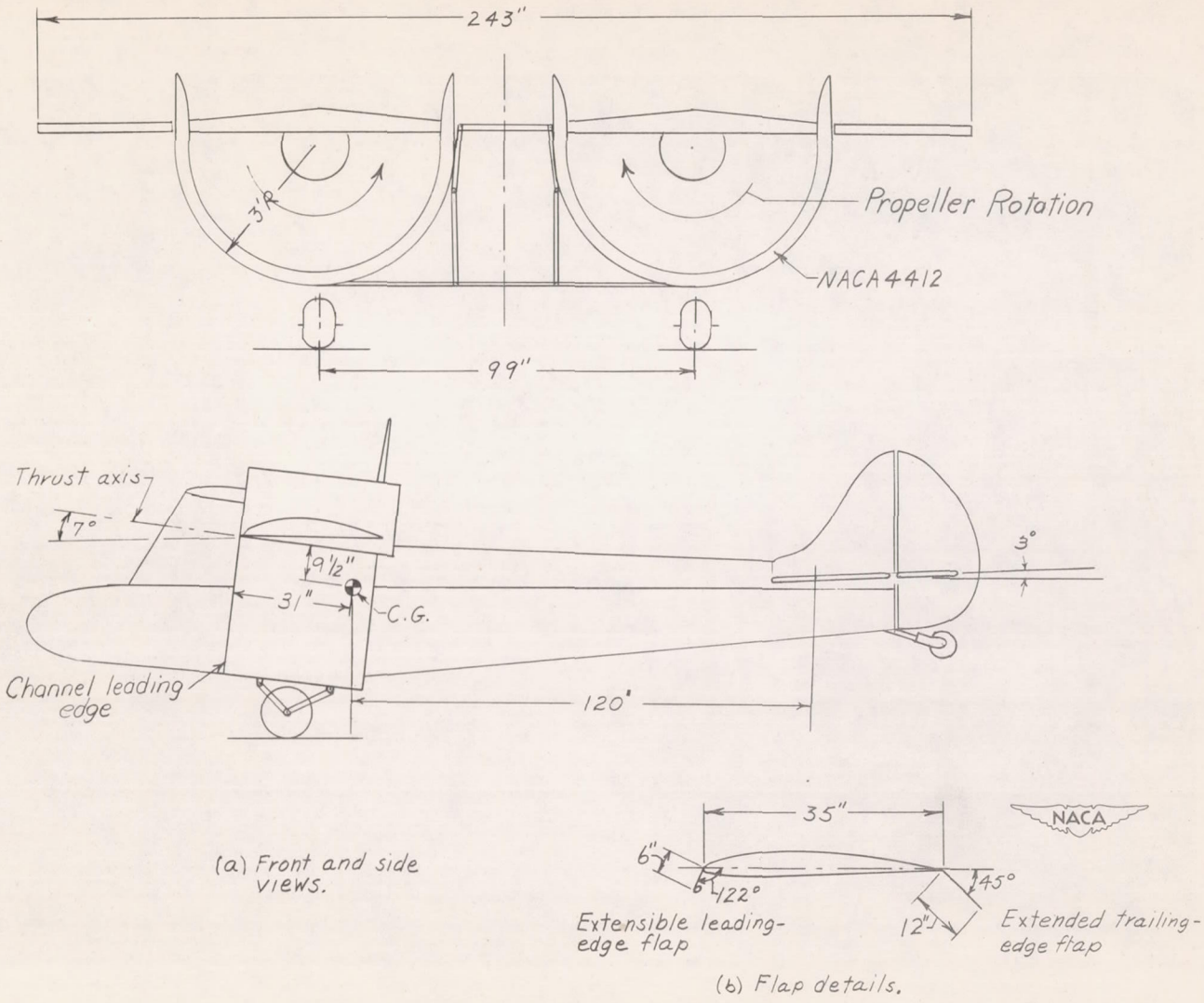

Figure 2.- General arrangement of the Custer Channel Wing airplane.

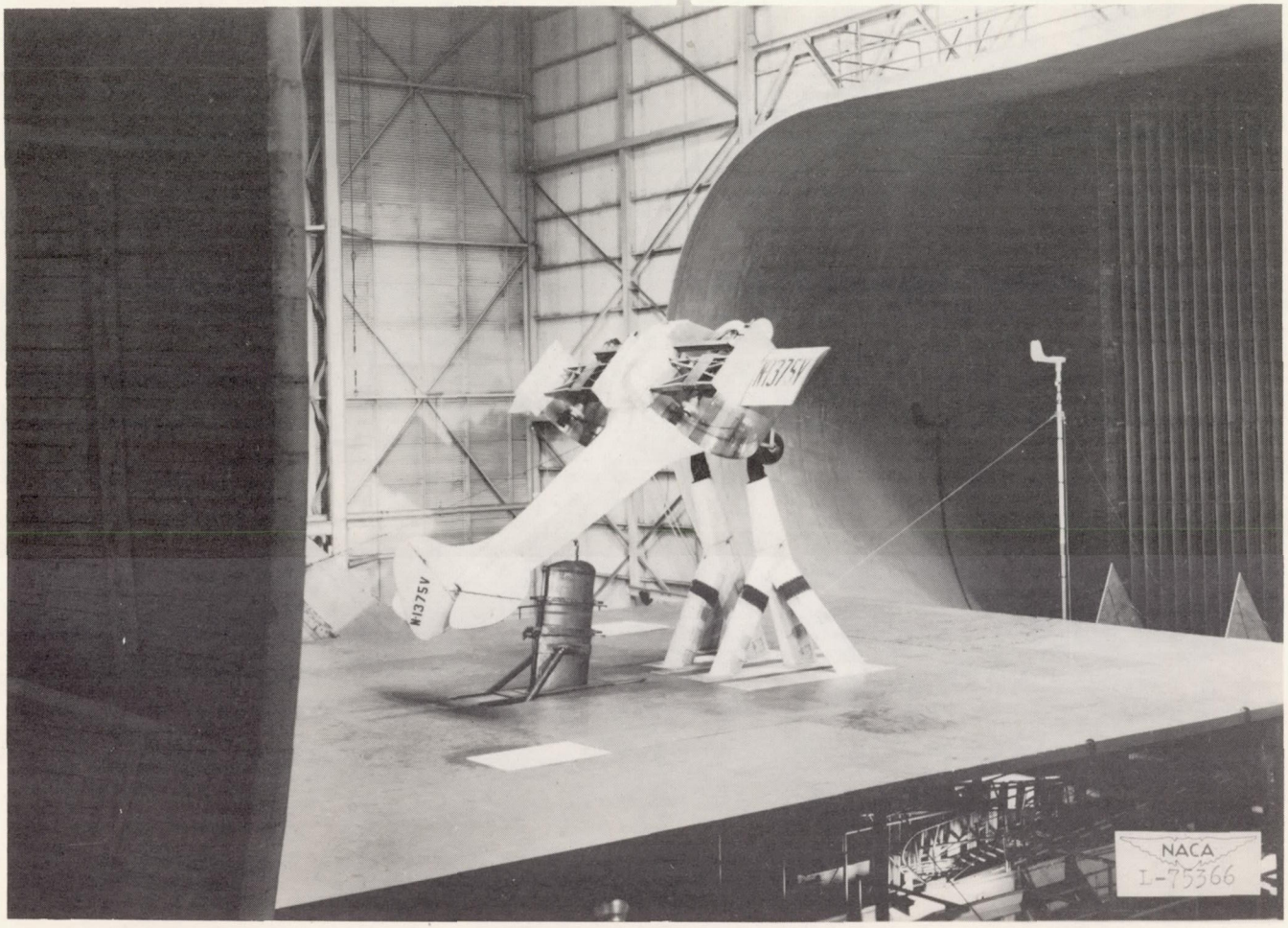

(a) Wind-tunnel arrangement.

Figure 3.- Langley full-scale-tunnel-test arrangements of the Custer Channel Wing airplane.

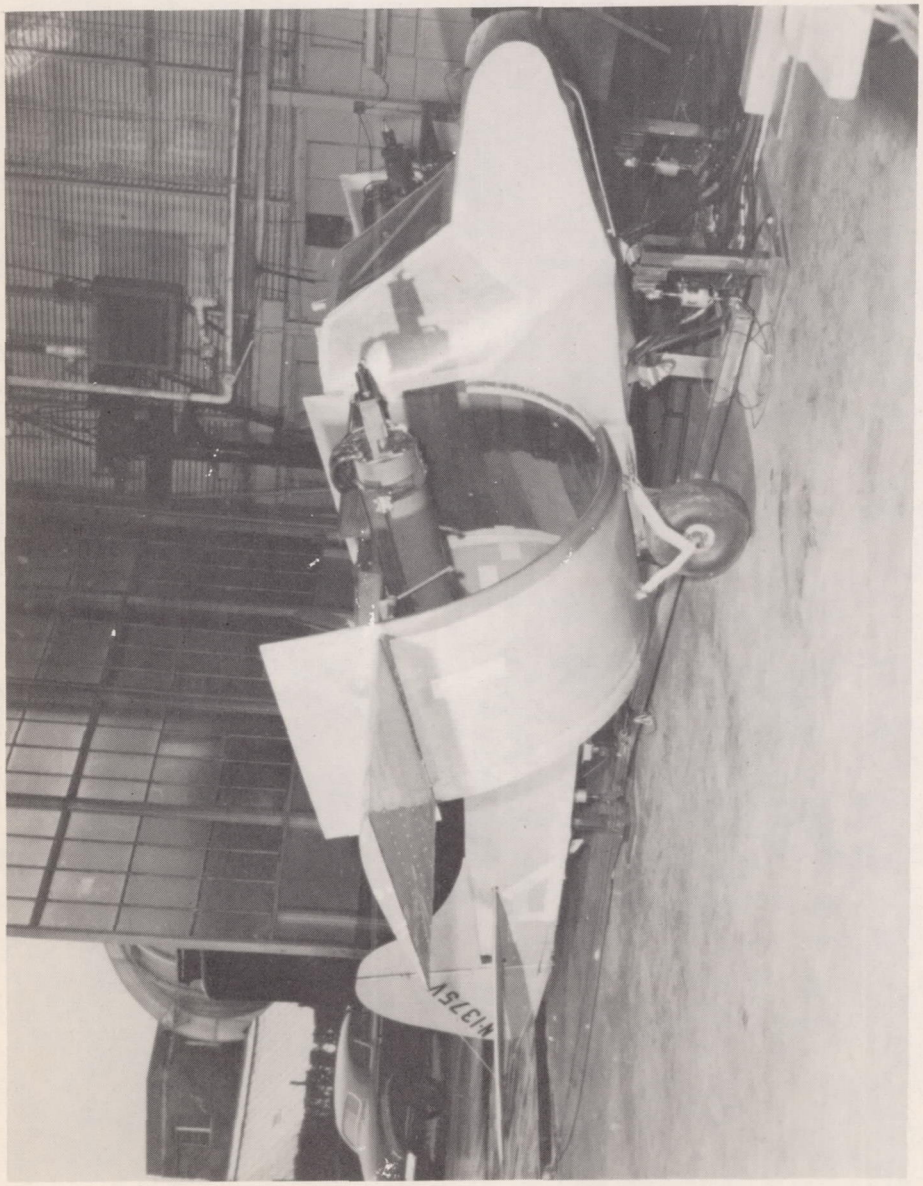

(b) Ground-test arrangement. L-77398

Figure 3.- Concluded.

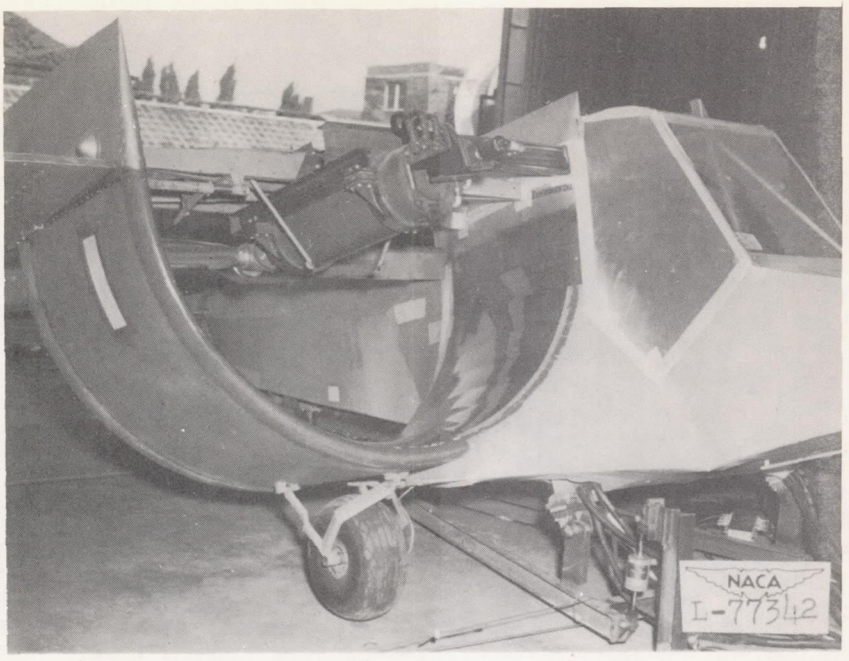

(a) Motor installation for original tests.

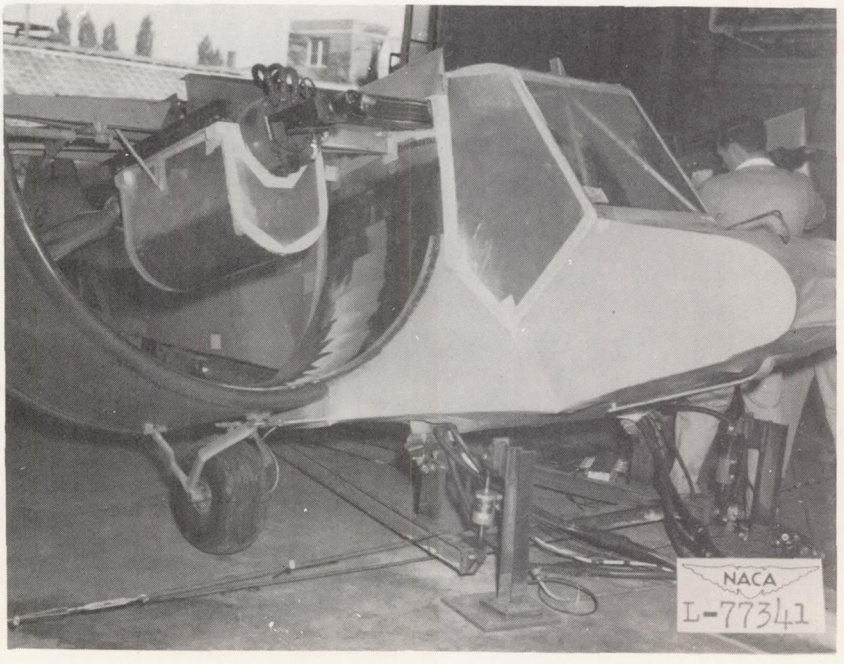

(b) Modified nacelle mock-up.

Figure 4.- Photographs of the original and modified electric-motor—nacelle installations on the Custer Channel Wing airplane.

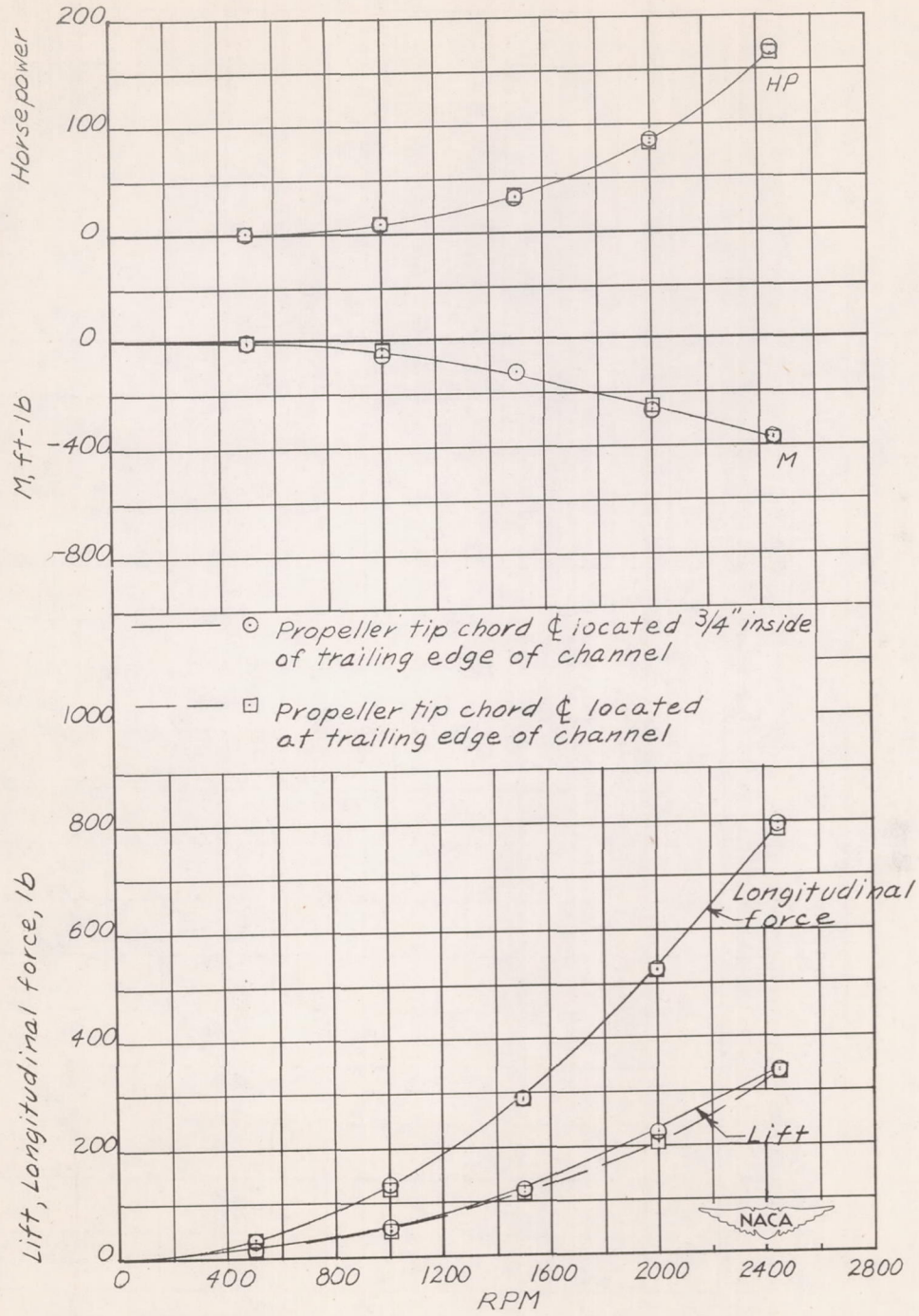

(a) Location of propeller in channel. ρ = 0.002326 slug/cu ft; q = 0 lb/sq ft.

Figure 5.- Effect of propeller rotational speed on the static or near-static characteristics of the Custer Channel Wing airplane in the absence of ground effect. $\delta_e = 0^\circ$; $\delta_r = 0^\circ$; $\alpha = 0^\circ$.

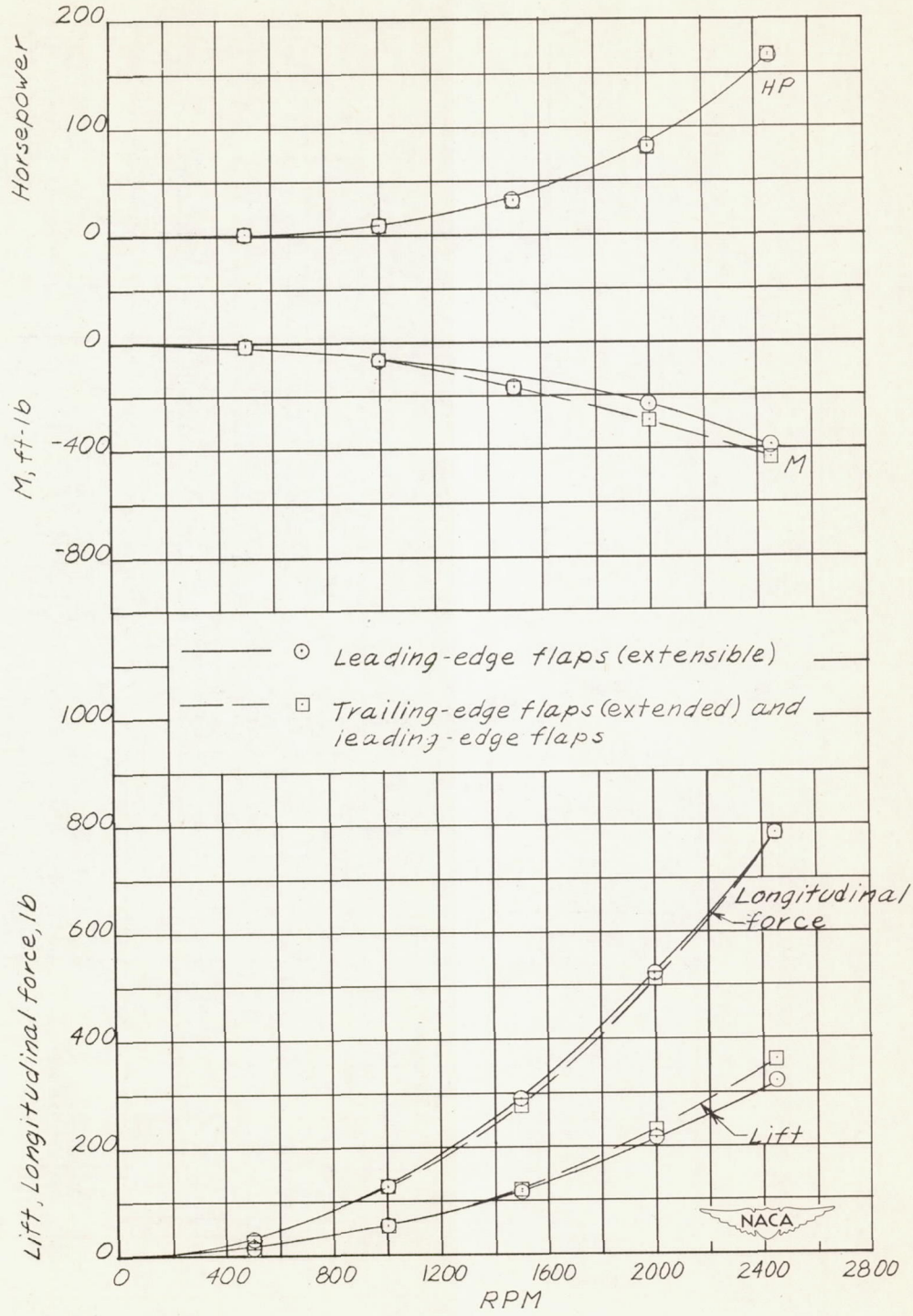

(b) Leading-edge and trailing-edge flaps installed. ρ = 0.002324 slug/cu ft; q = 0 lb/sq ft.

Figure 5.- Continued.

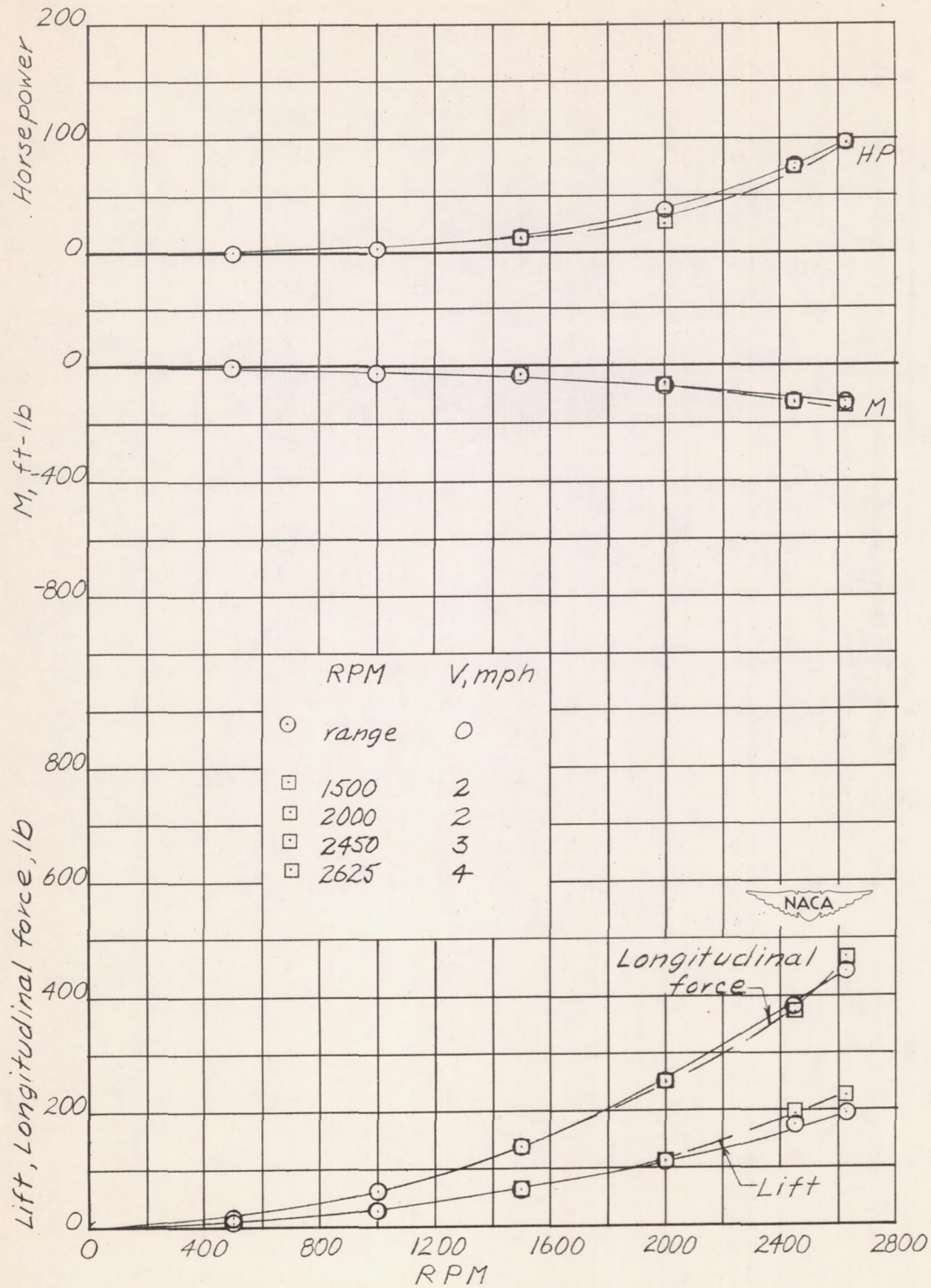

(c) Port motor operating. ρ = 0.002328 slug/cu ft.

Figure 5.- Concluded.

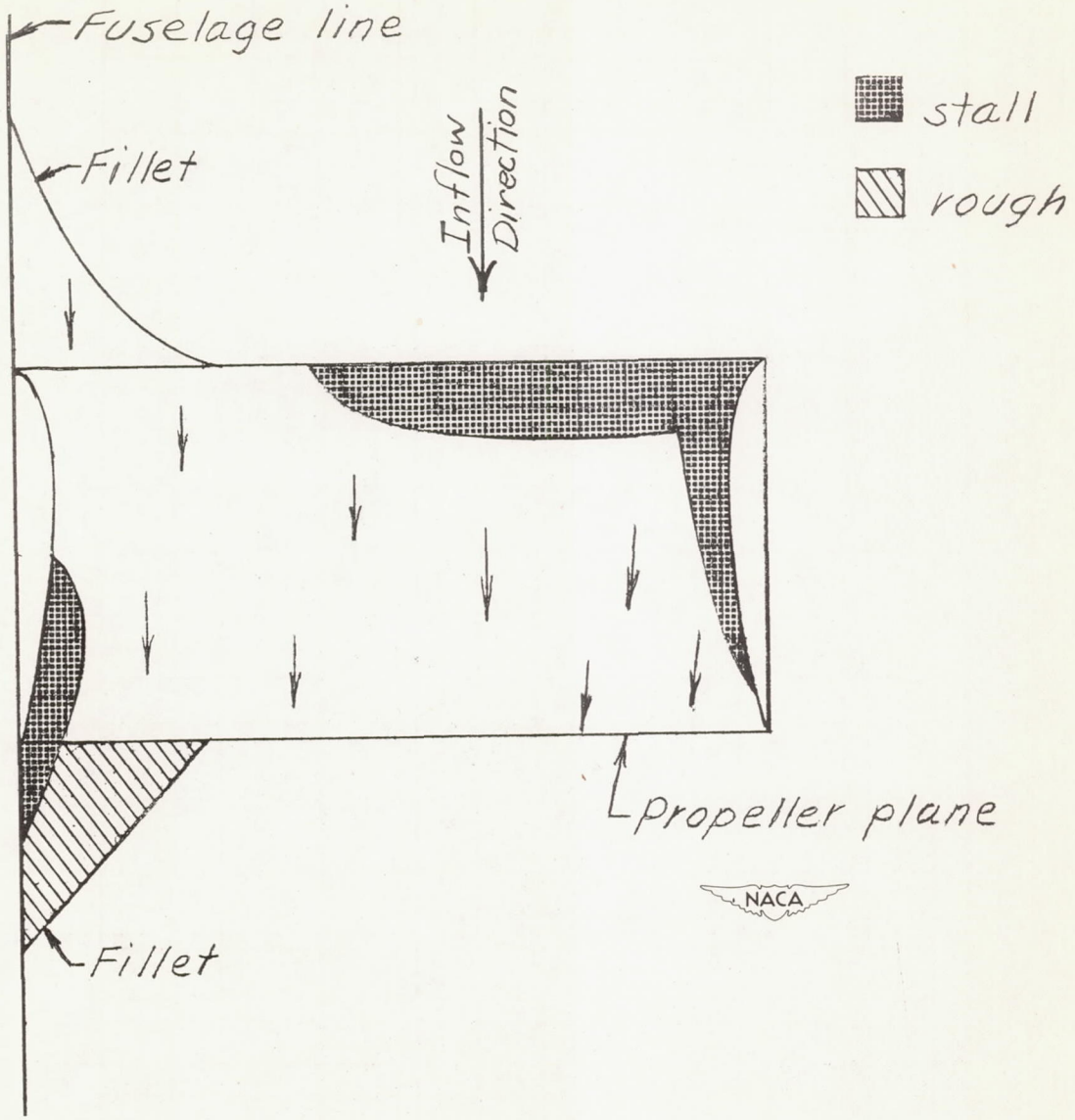

Figure 6.- Stalling characteristics of the Custer Channel Wing airplane in the absence of ground effect. Propellers operating at 2,450 rpm. q = 0 lb/sq ft.

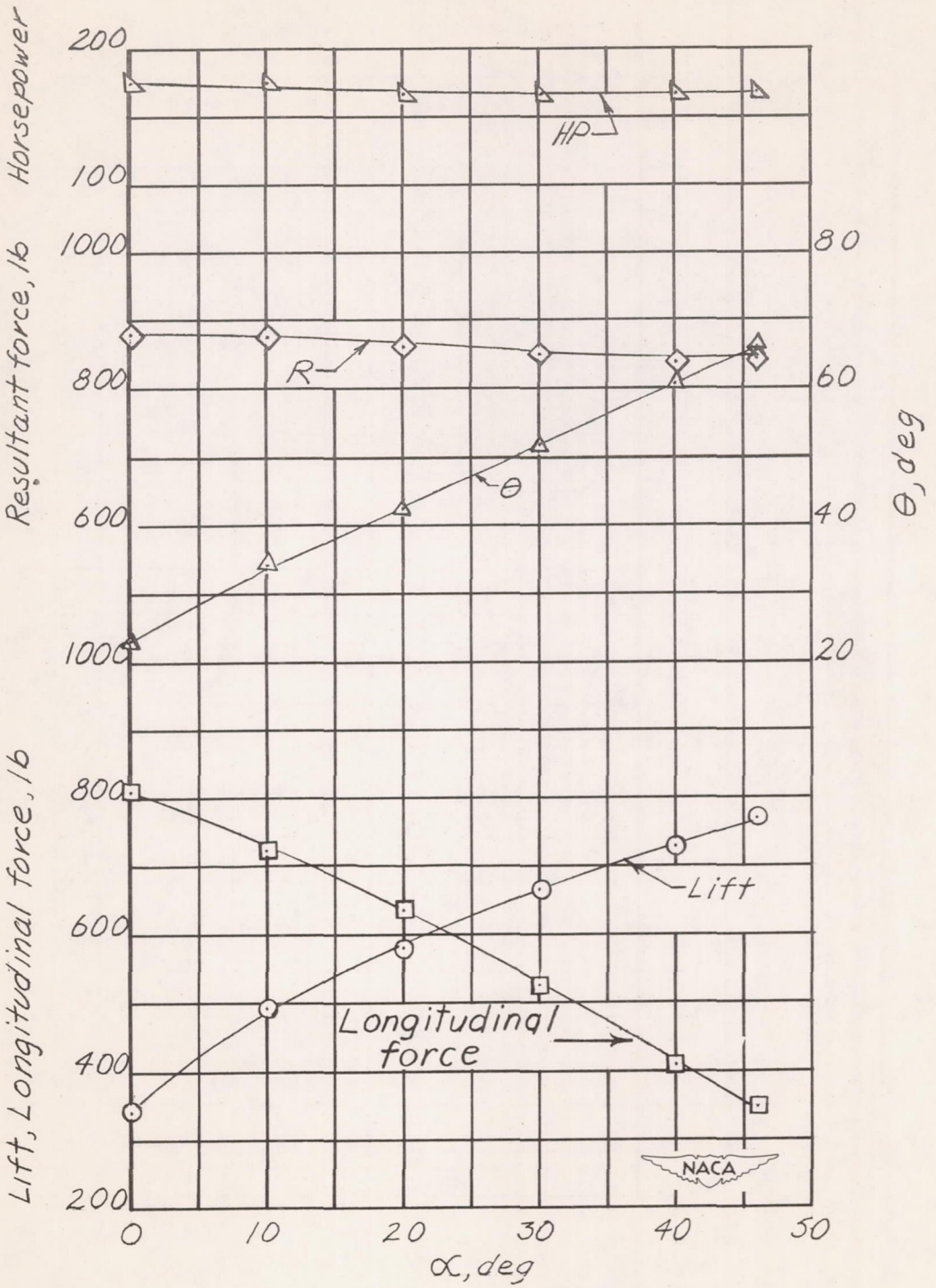

Figure 7.- Effect of inclination of thrust axis on the static characteristics of the Custer Channel Wing airplane in the absence of ground effect. Propellers operating at 2,450 rpm; configuration untrimmed in pitch. $q = 0$ lb/sq ft; $\delta_e = -10^\circ$.

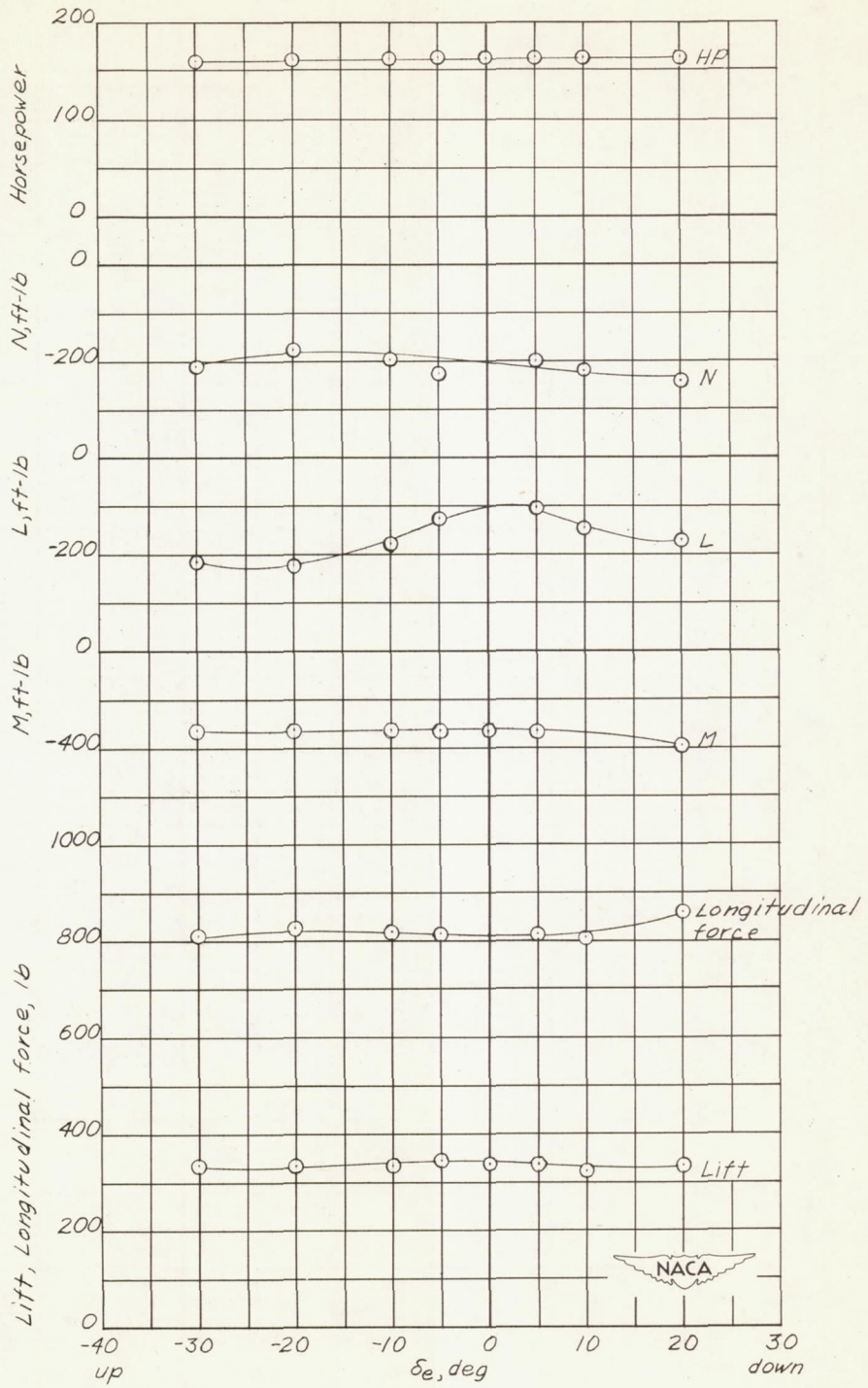

(a) $\alpha = 0^\circ$; $\delta_r = 0^\circ$; $\rho = 0.002308$ slug/cu ft.

Figure 8.- Effect of control-surface deflection on the static characteristics of the Custer Channel Wing airplane in the absence of ground effect. Propellers operating at 2,450 rpm. q = 0 lb/sq ft.

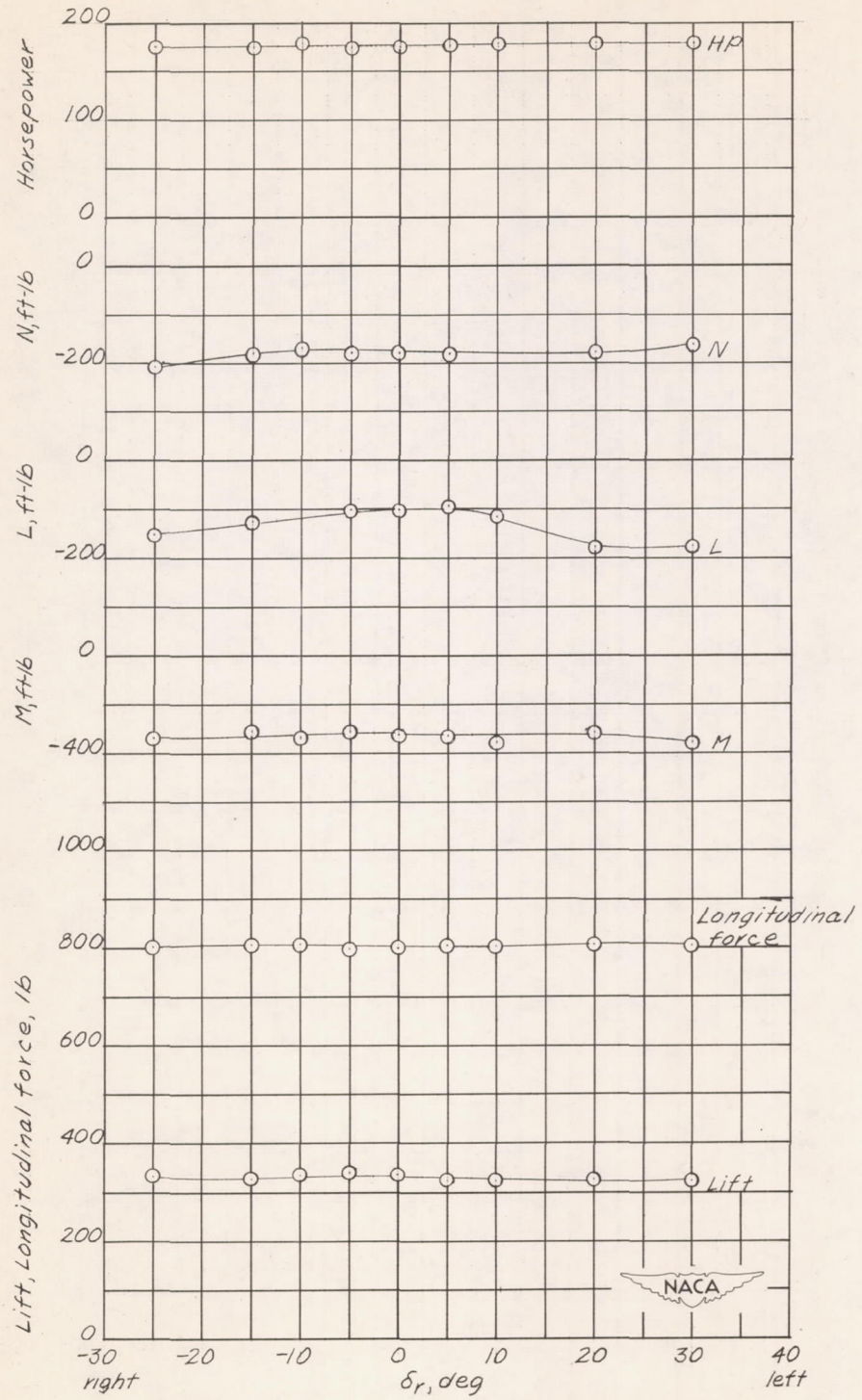

(b) $\alpha = 0^{\circ}$; $\delta_e = 0^{\circ}$; $\rho = 0.002308$ slug/cu ft.

Figure 8.- Continued.

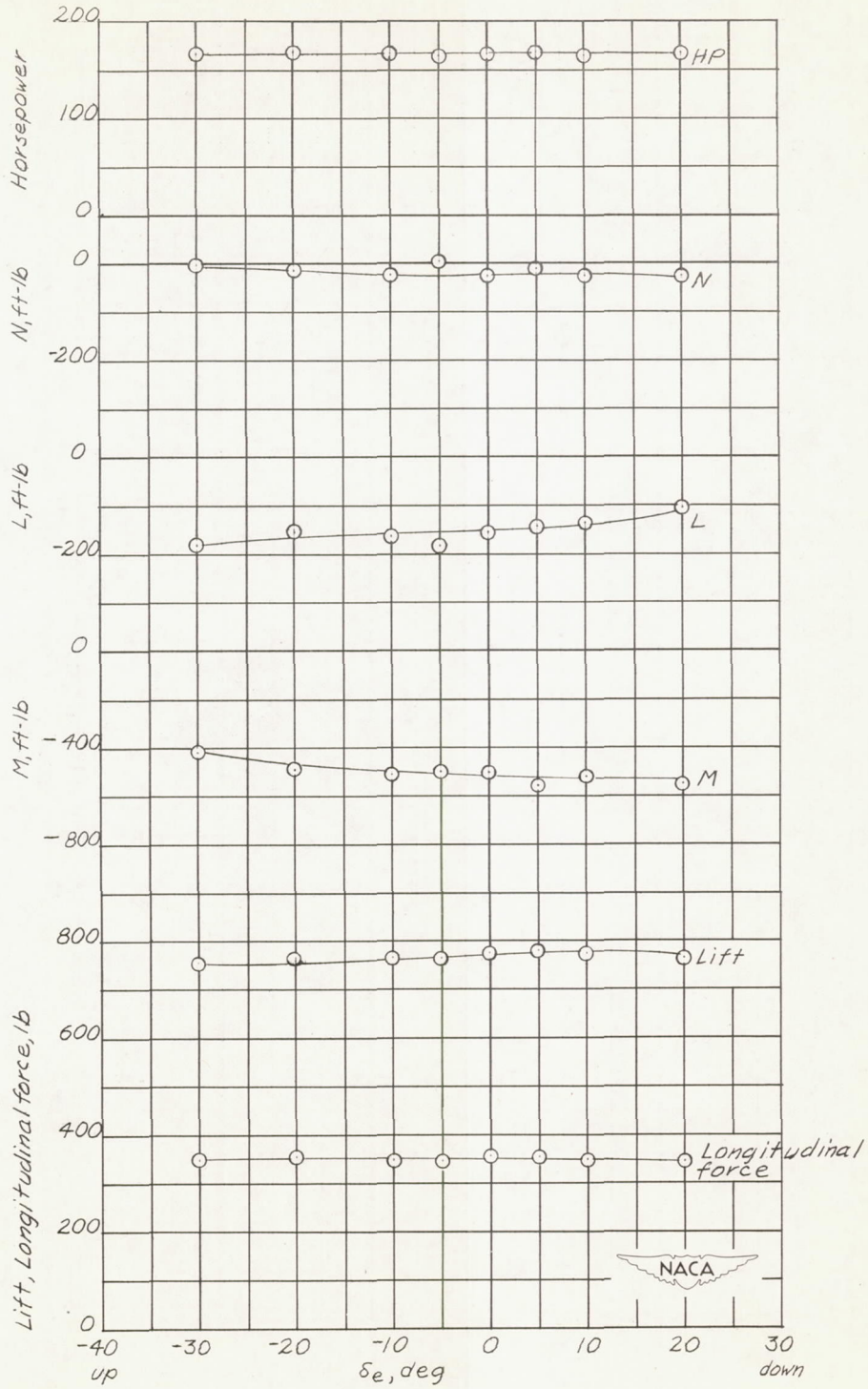

(c) $\alpha = 46^{\circ}$; $\delta_r = 0^{\circ}$; $\rho = 0.002312$ slug/cu ft.

Figure 8.- Continued.

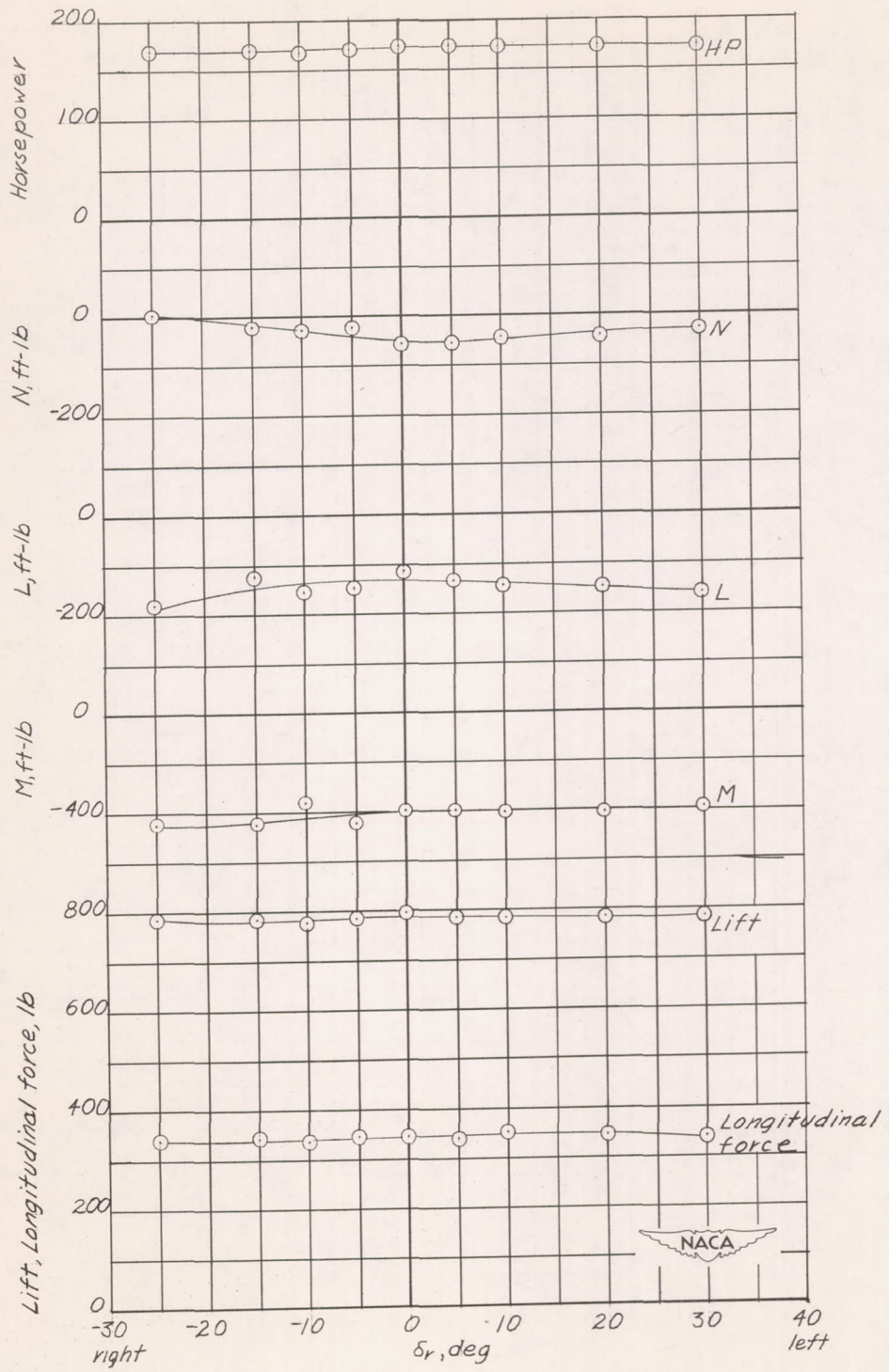

(d) $\alpha = 46^{\circ}$; $\delta_e = 0^{\circ}$; $\rho = 0.002312$ slug/cu ft.

Figure 8.- Concluded.

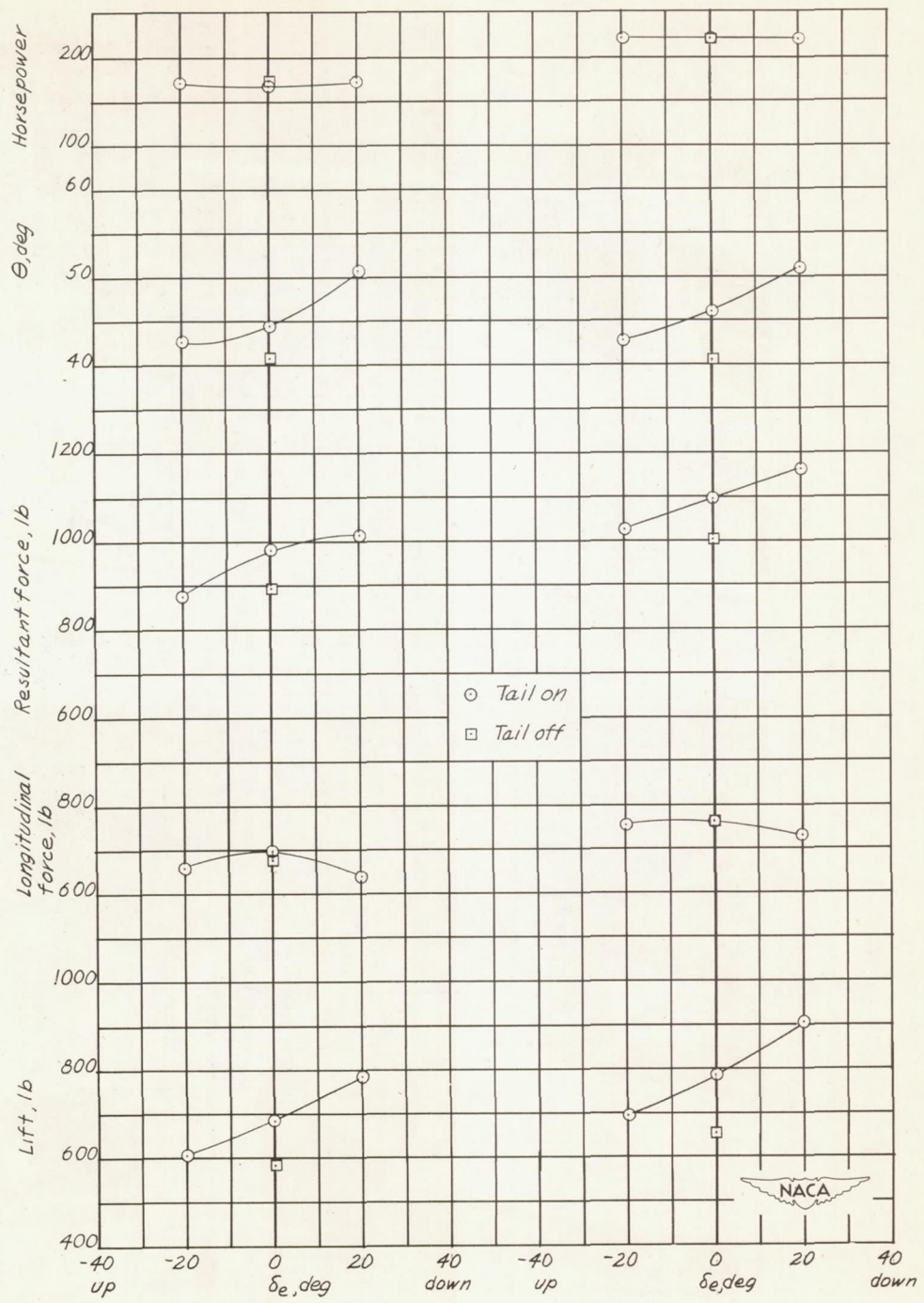

(a) 2,450 rpm. (b) 2,625 rpm.

Figure 9.- Effect of the horizontal tail on the static characteristics of the Custer Channel Wing airplane in the presence of a ground boundary. Propellers operating; basic electric-motor nacelle. q = 0 lb/sq ft.

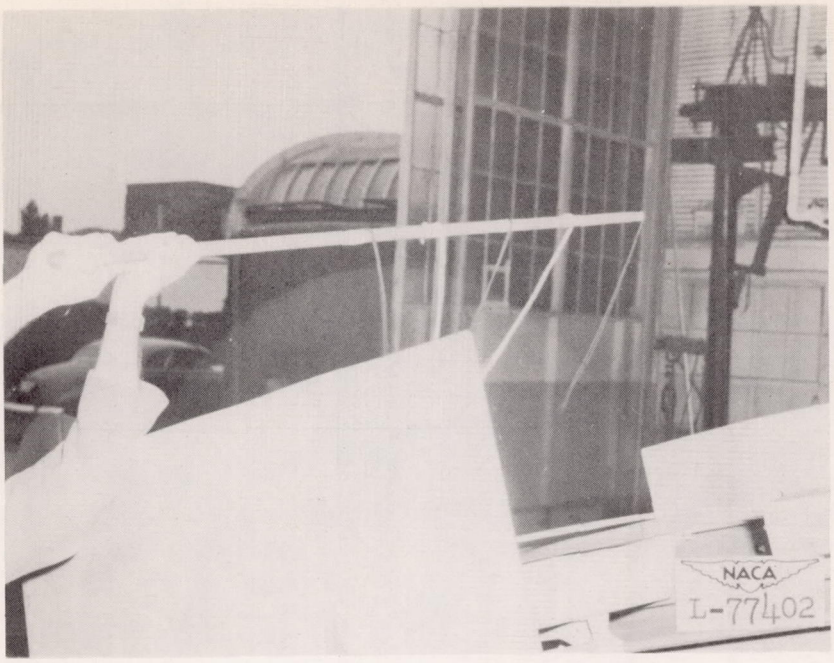

(a) Above and in front of the propeller disk.

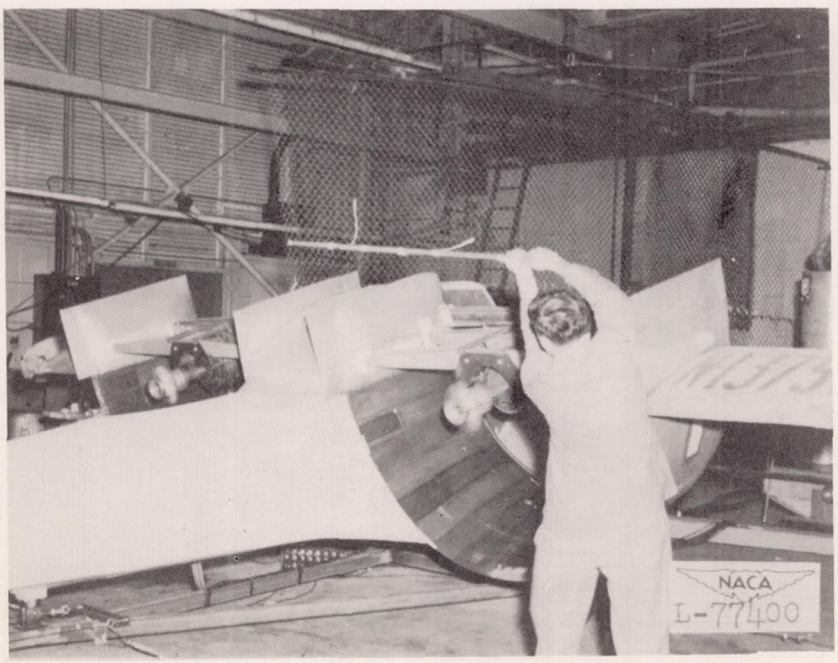

(b) Behind the propeller disk near the tip radius.

Figure 10.- Flow studies of the Custer Channel Wing airplane in the static ground tests. Propellers operating at 2,450 rpm. $\alpha \approx 19^{\circ}$; $\delta_e = 0^{\circ}$.

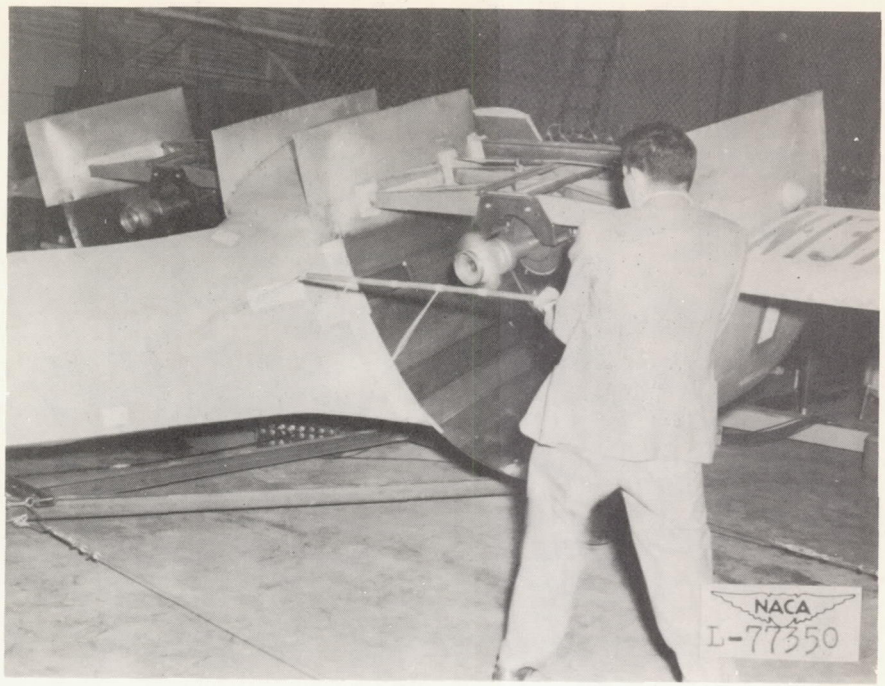

(c) Behind the propeller on the center line of nacelle.

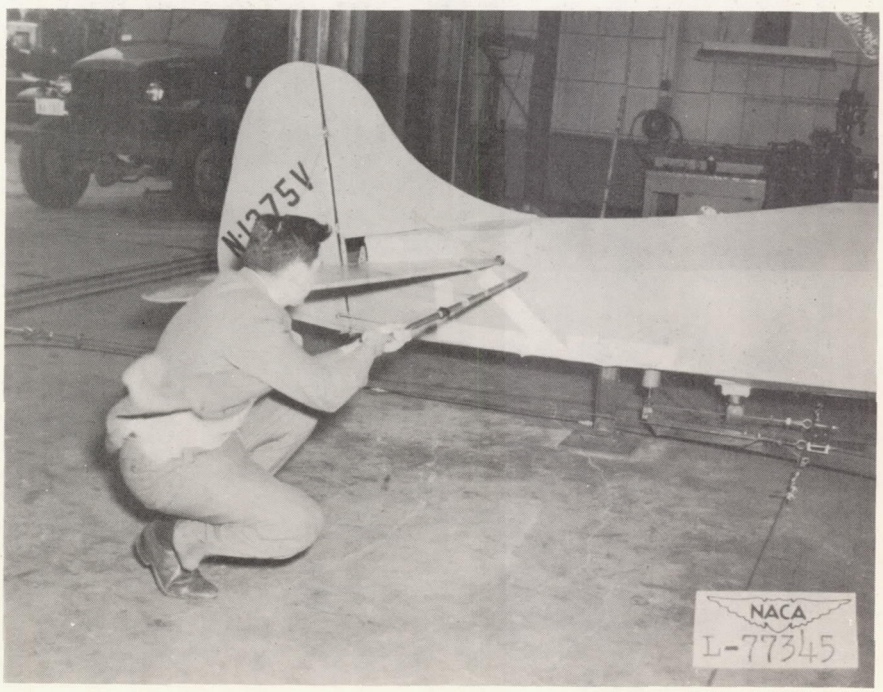

(d) Ahead of horizontal tail.

Figure 10.- Concluded.

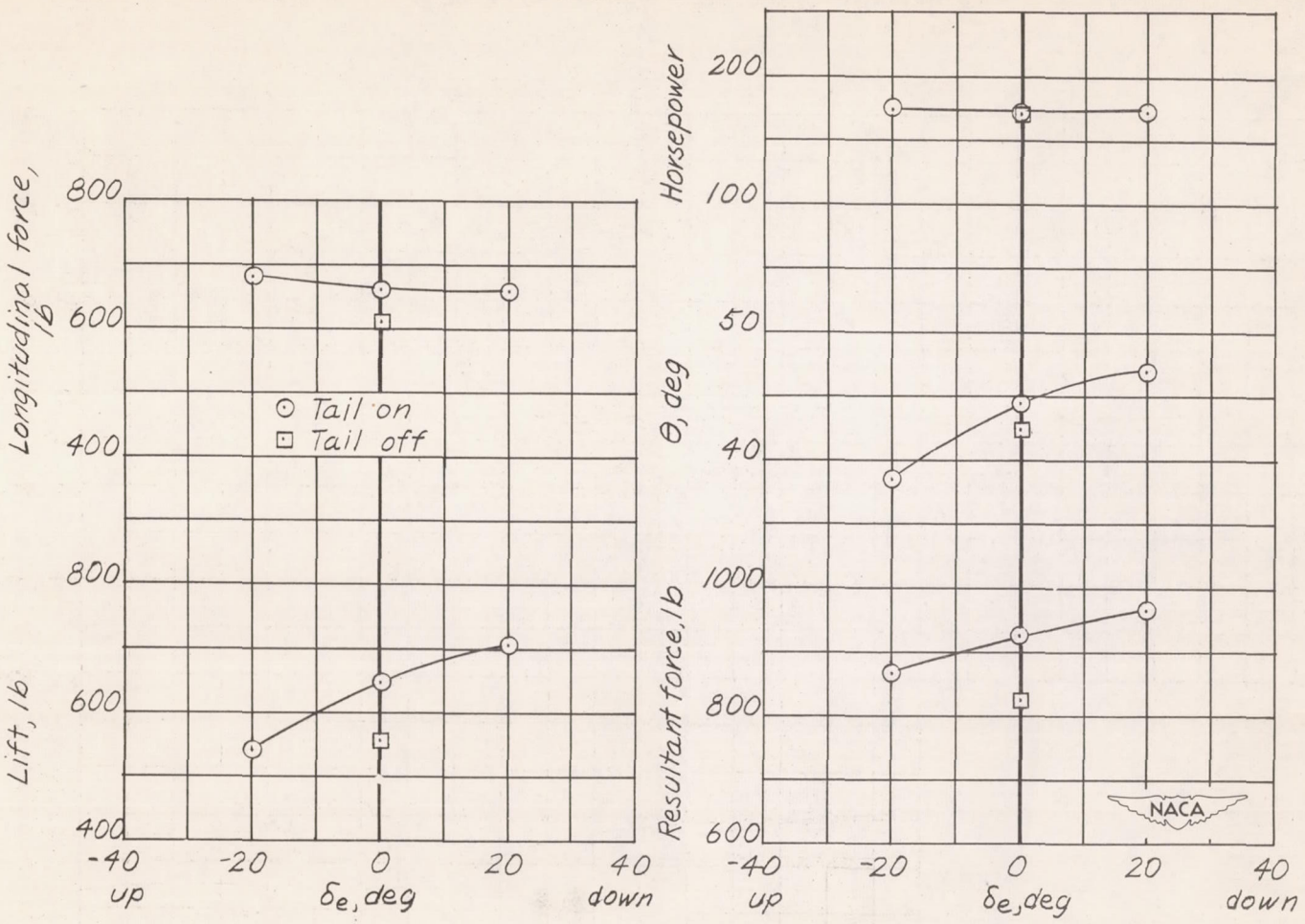

Figure 11.- Effect of horizontal tail on the static characteristics of the Custer Channel Wing airplane in the presence of a ground boundary. Propellers operating at 2,450 rpm; modified nacelle mock-up. q = 0 lb/sq ft.

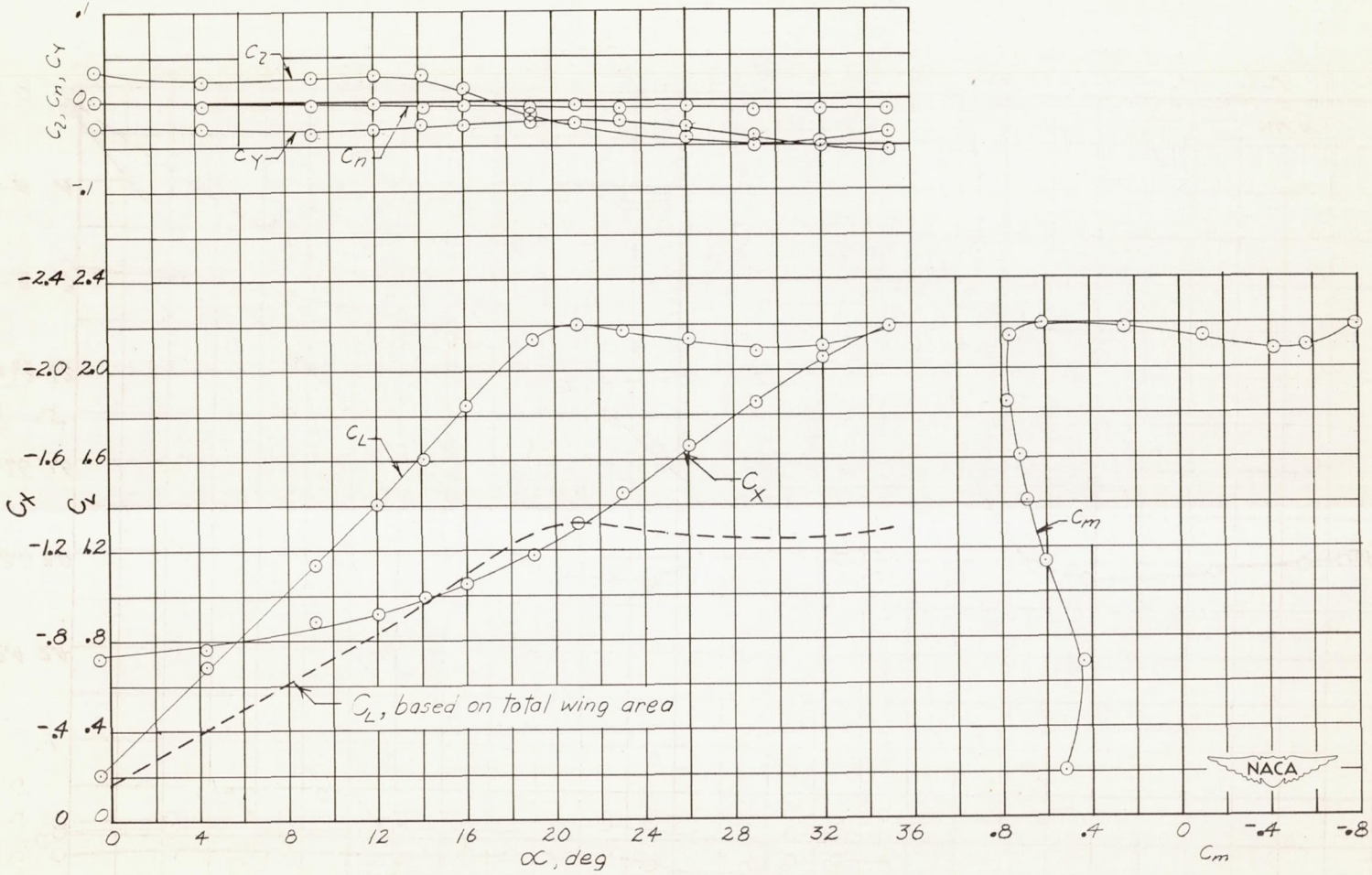

(a) q_{av} = 1.73 lb/sq ft; ρ = 0.002280 slug/cu ft.

Figure 12.- Aerodynamic characteristics of the Custer Channel Wing airplane. Propellers removed. $\delta_e = 0^\circ$; $\delta_r = 0^\circ$.

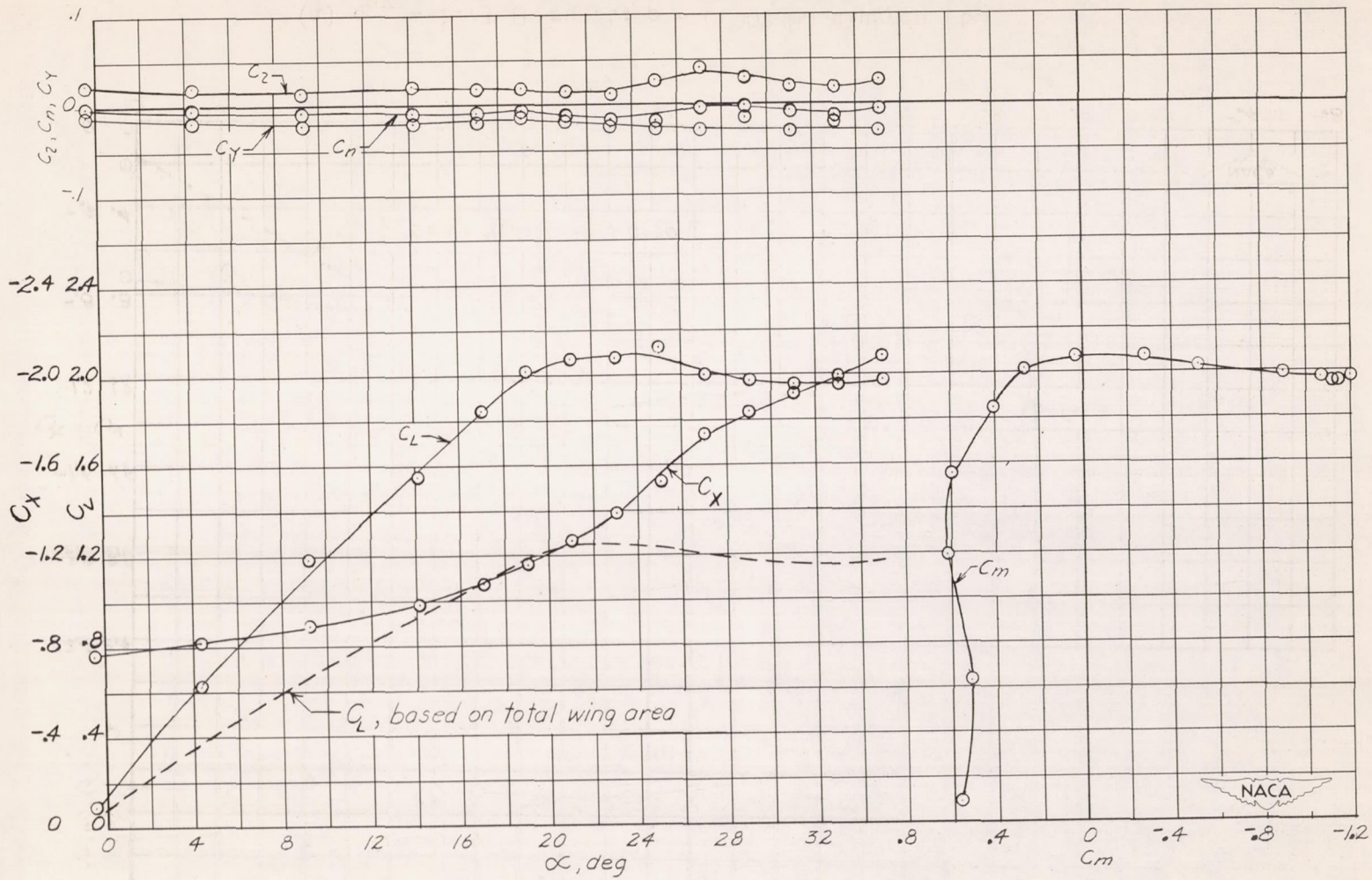

(b) q_{av} = 3.97 lb/sq ft; ρ = 0.002272 slug/cu ft.

Figure 12.- Concluded.

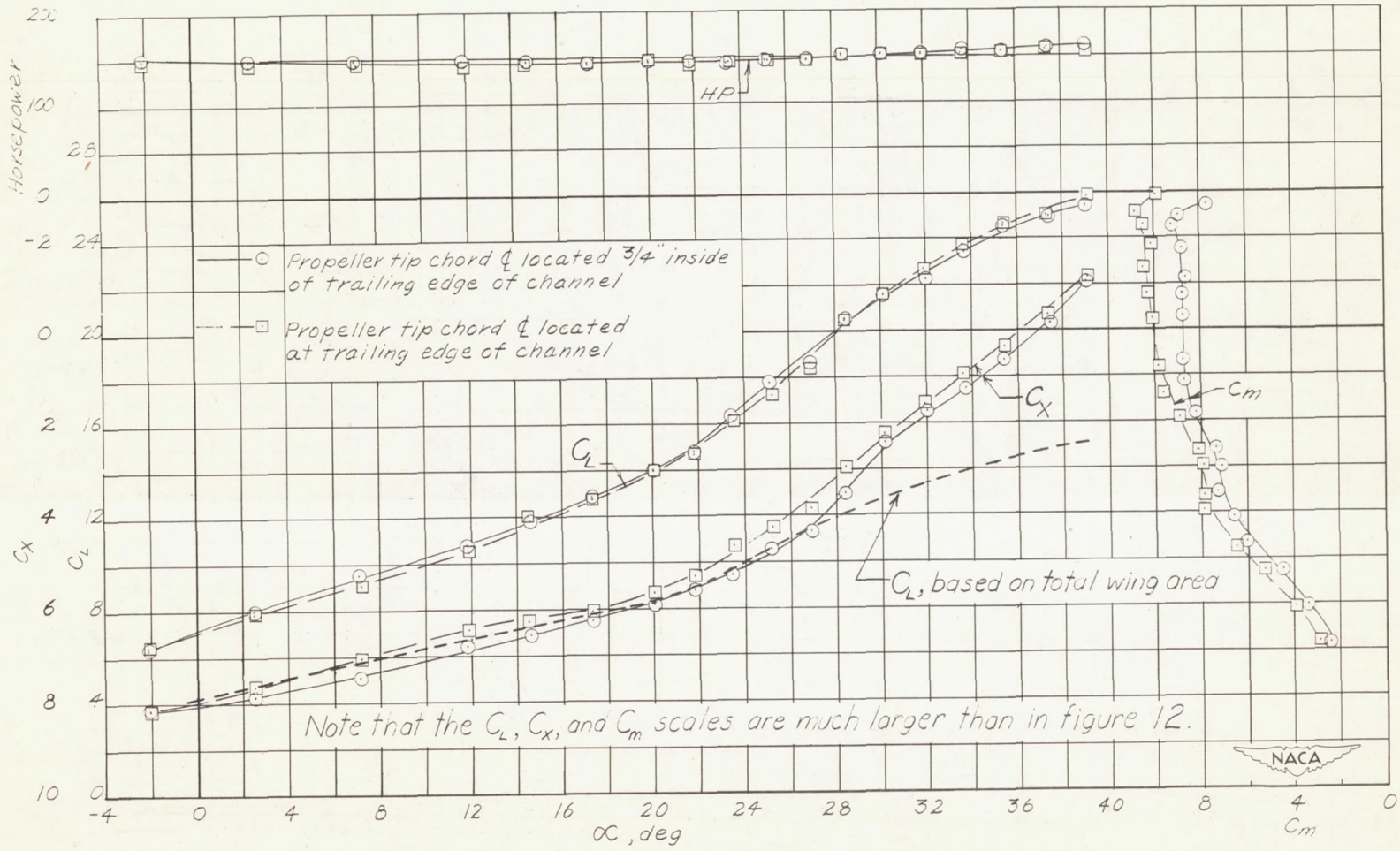

(a) q_{av} = 1.89 lb/sq ft; ρ = 0.002307 slug/cu ft.

Figure 13.- Aerodynamic characteristics of the Custer Channel Wing airplane. Propellers operating at 2,450 rpm. $\delta_e = 0^\circ$; $\delta_r = 0^\circ$.

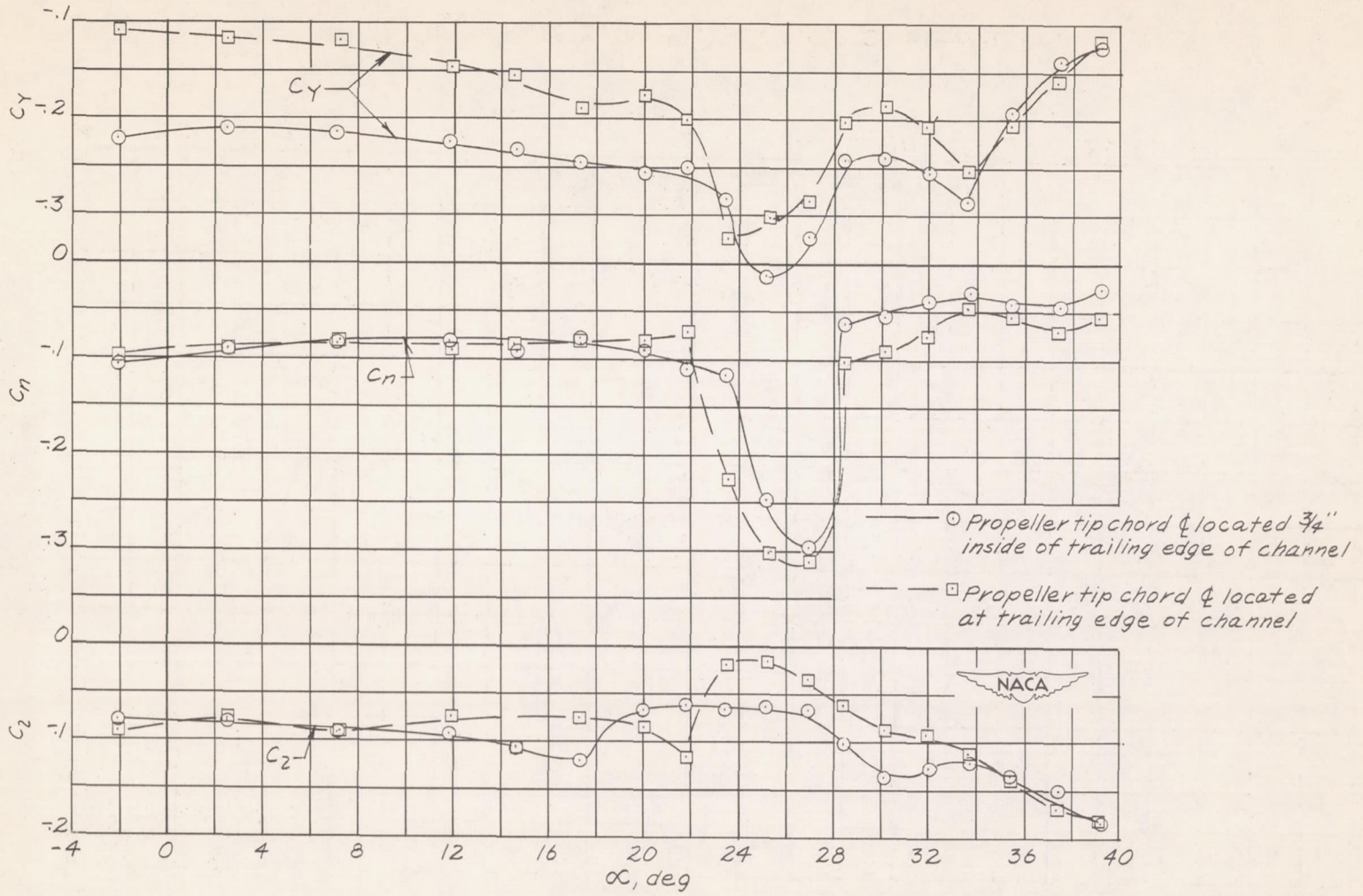

(a) Concluded.

Figure 13.- Continued.

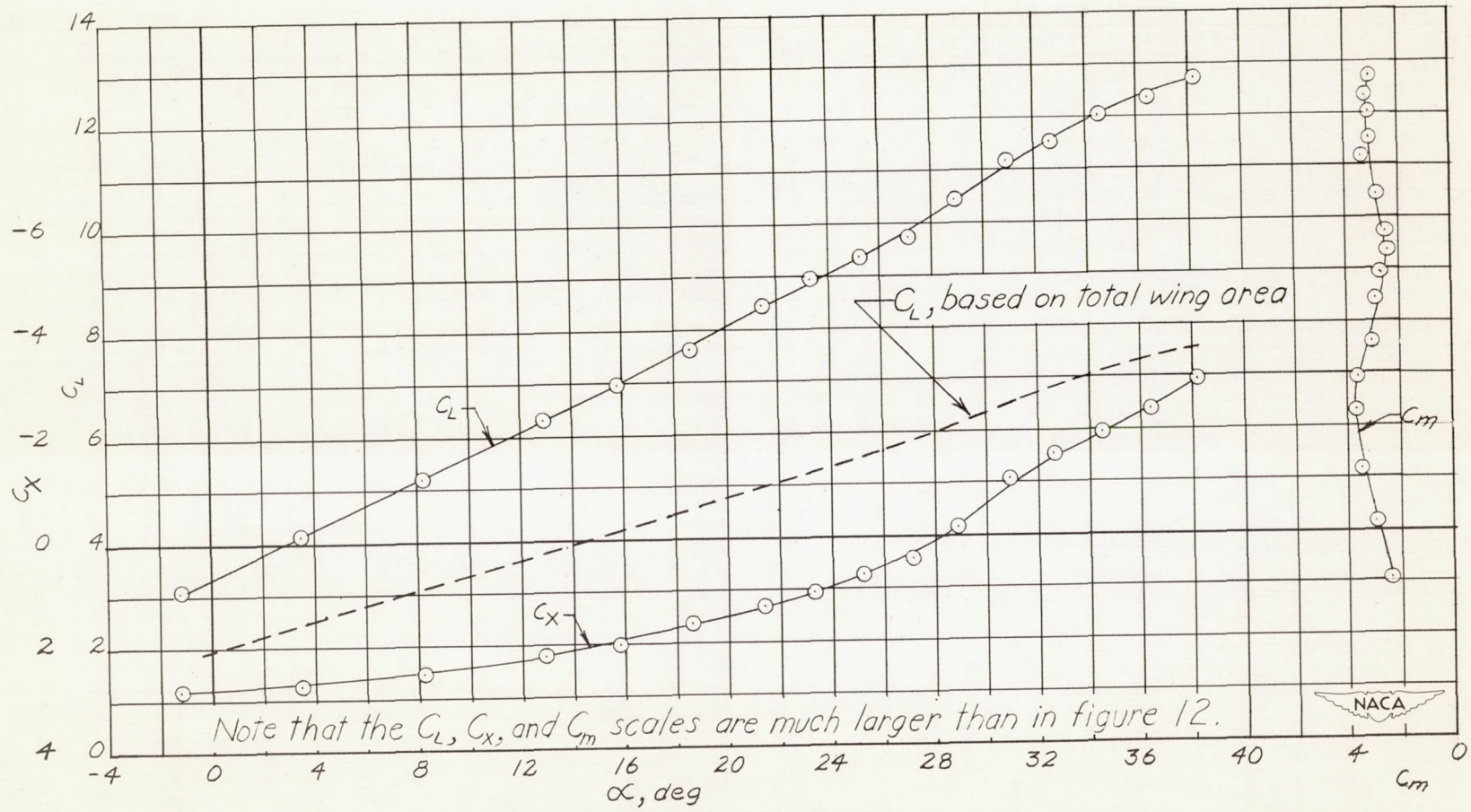

(b) q_{av} = 4.22 lb/sq ft; ρ = 0.002320 slug/cu ft.

Figure 13.- Continued.

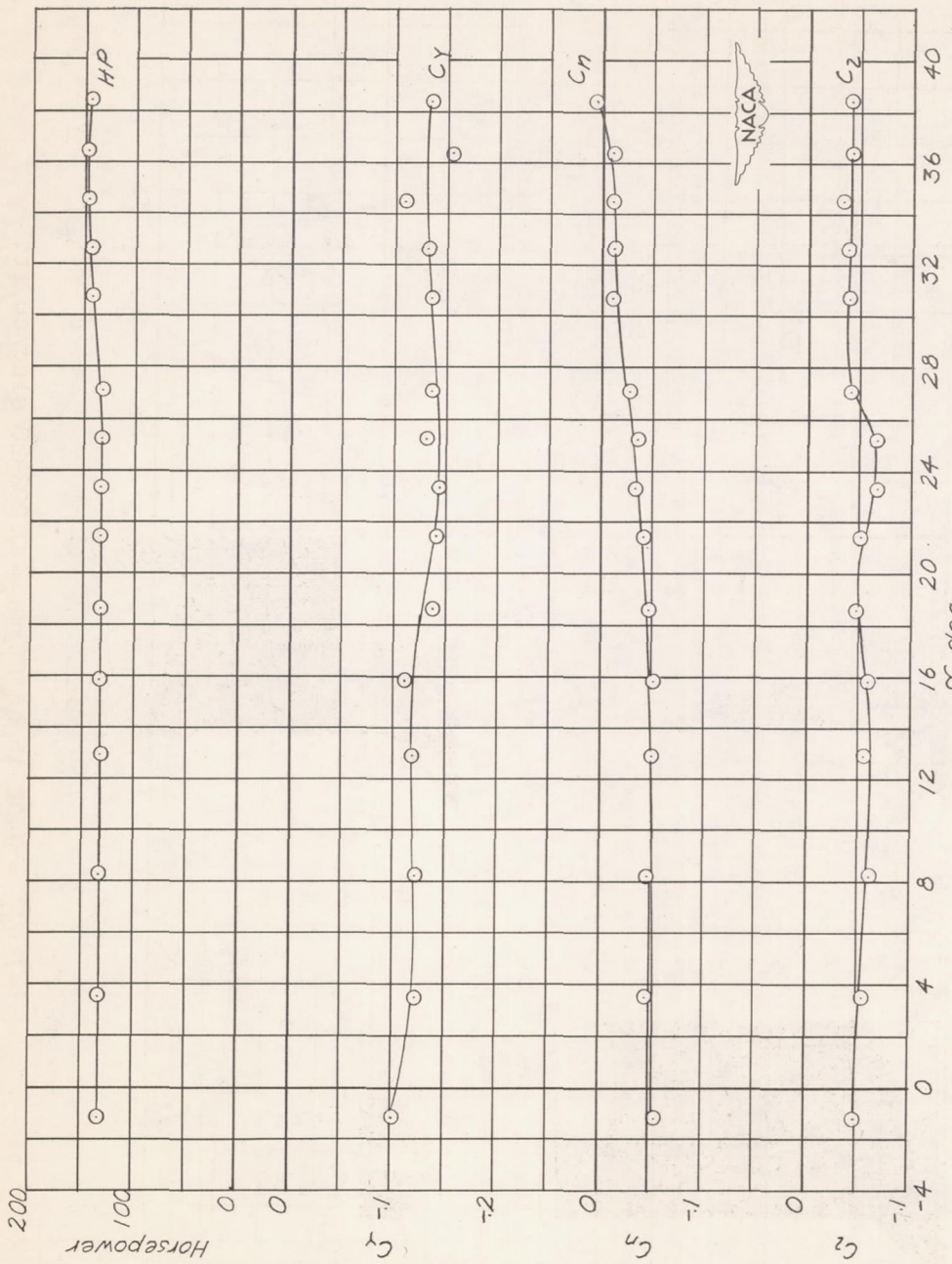

(b) Concluded.

Figure 13.- Concluded.

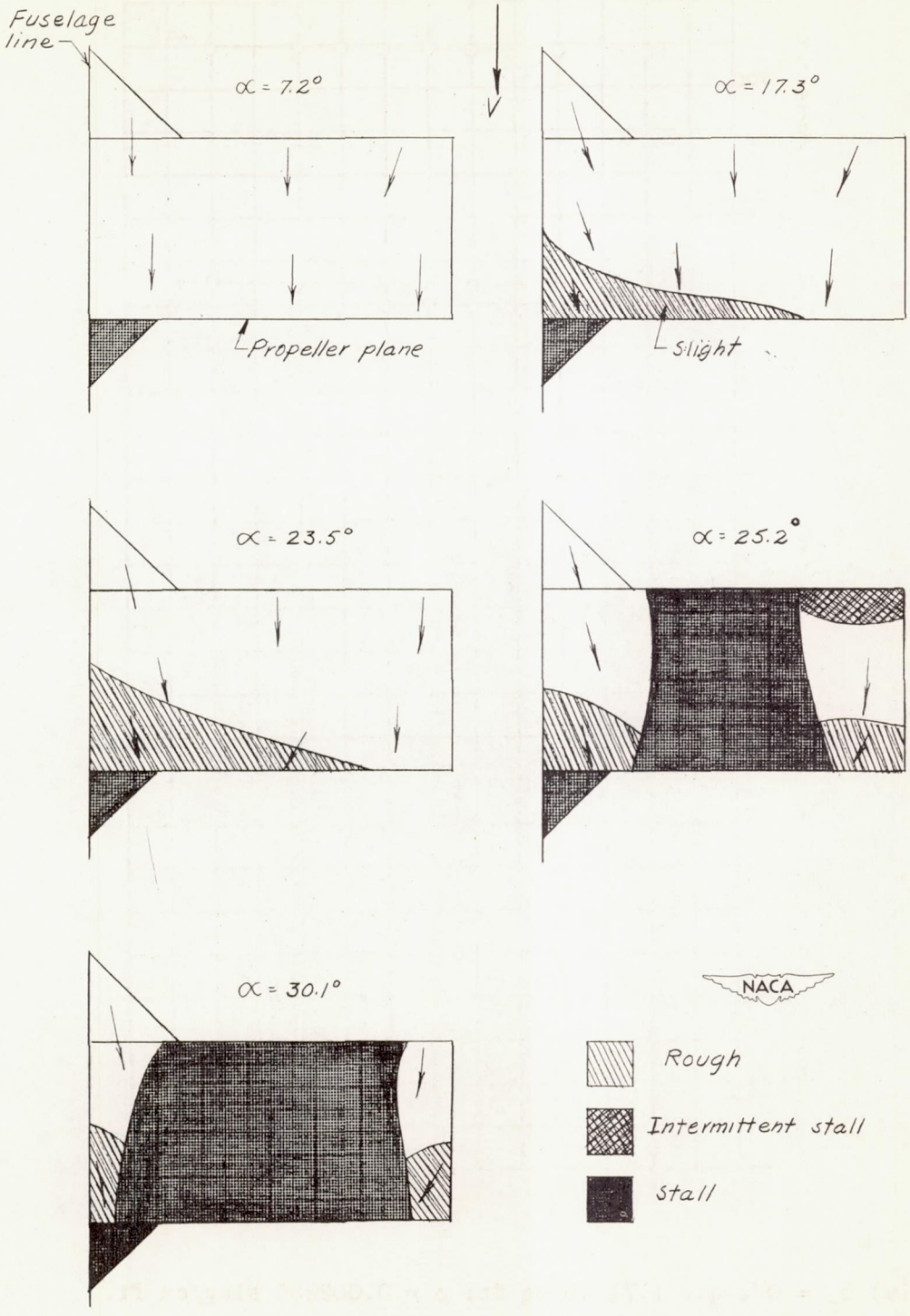

Figure 14.- Stalling characteristics of the Custer Channel Wing airplane. Propellers operating at 2,450 rpm. $\delta_e = 0^\circ$; $\delta_r = 0^\circ$; q = 1.74 lb/sq ft; ρ = 0.002323 slug/cu ft.

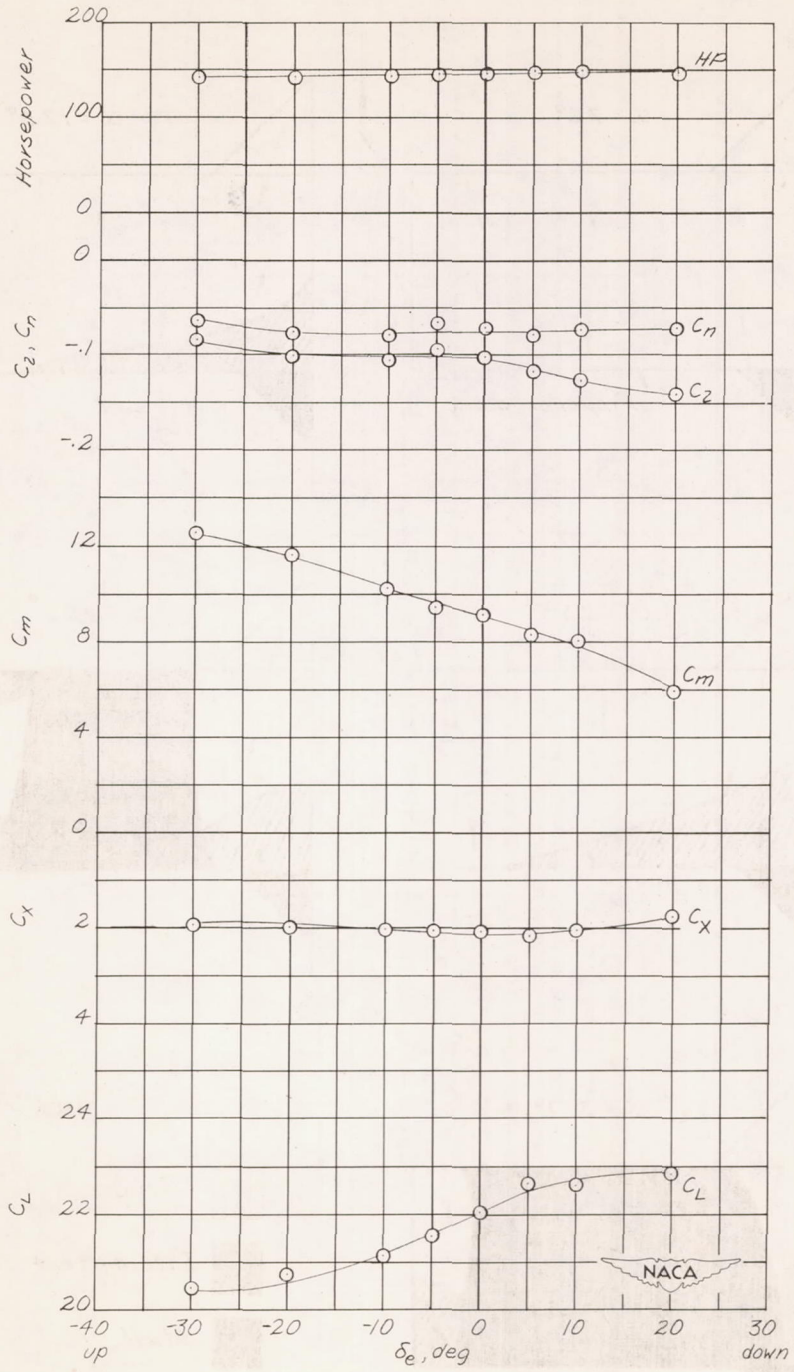

(a) $\delta_r = 0^\circ$; q = 1.71 lb/sq ft; ρ = 0.002280 slug/cu ft.

Figure 15.- Effect of control deflection on the aerodynamic characteristics of the Custer Channel Wing airplane. Propellers operating at 2,450 rpm. $\alpha = 31.1^\circ$.

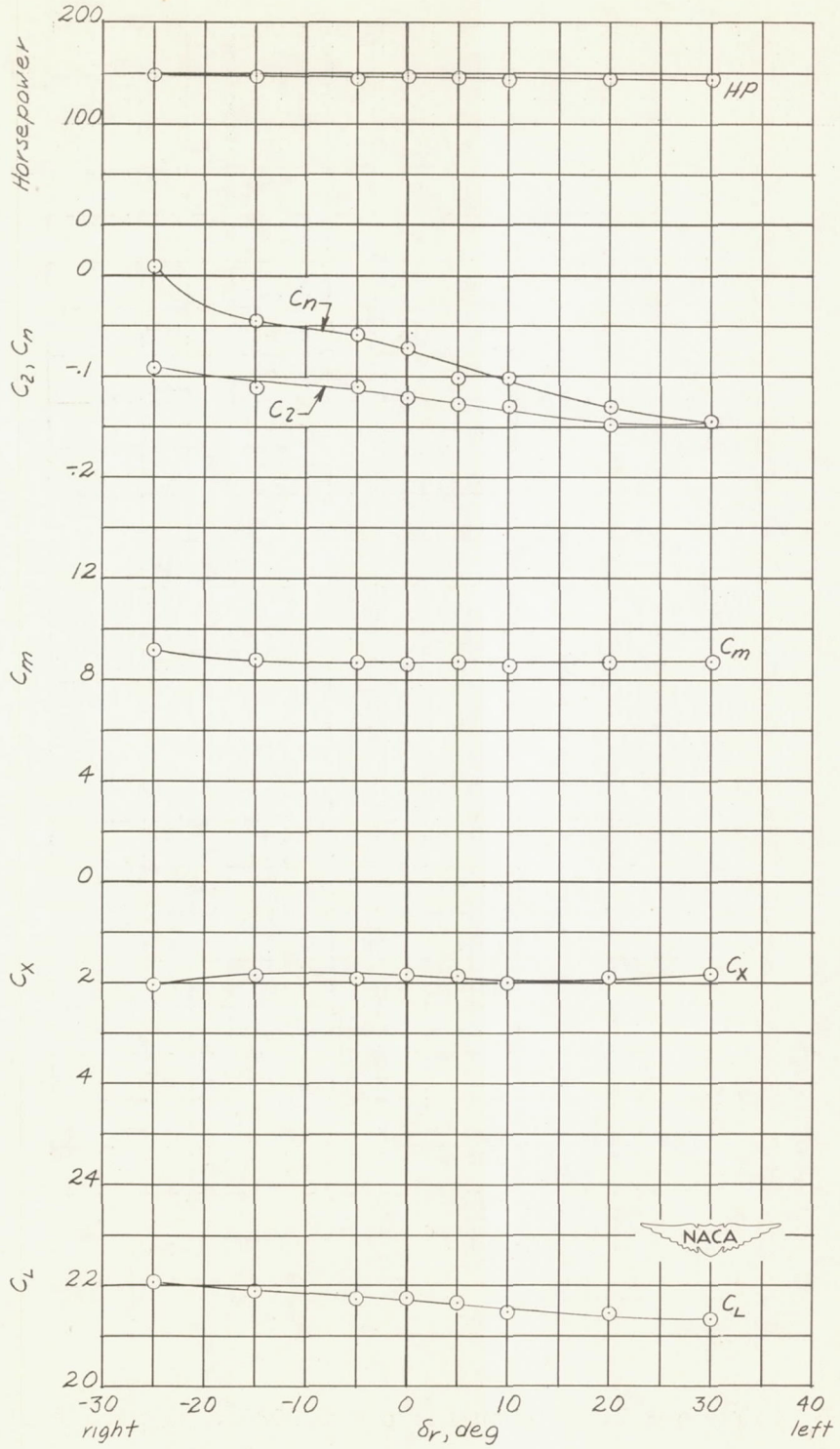

(b) $\delta_e = 0^\circ$; q = 1.71 lb/sq ft; ρ = 0.002270 slug/cu ft.

Figure 15.- Concluded.

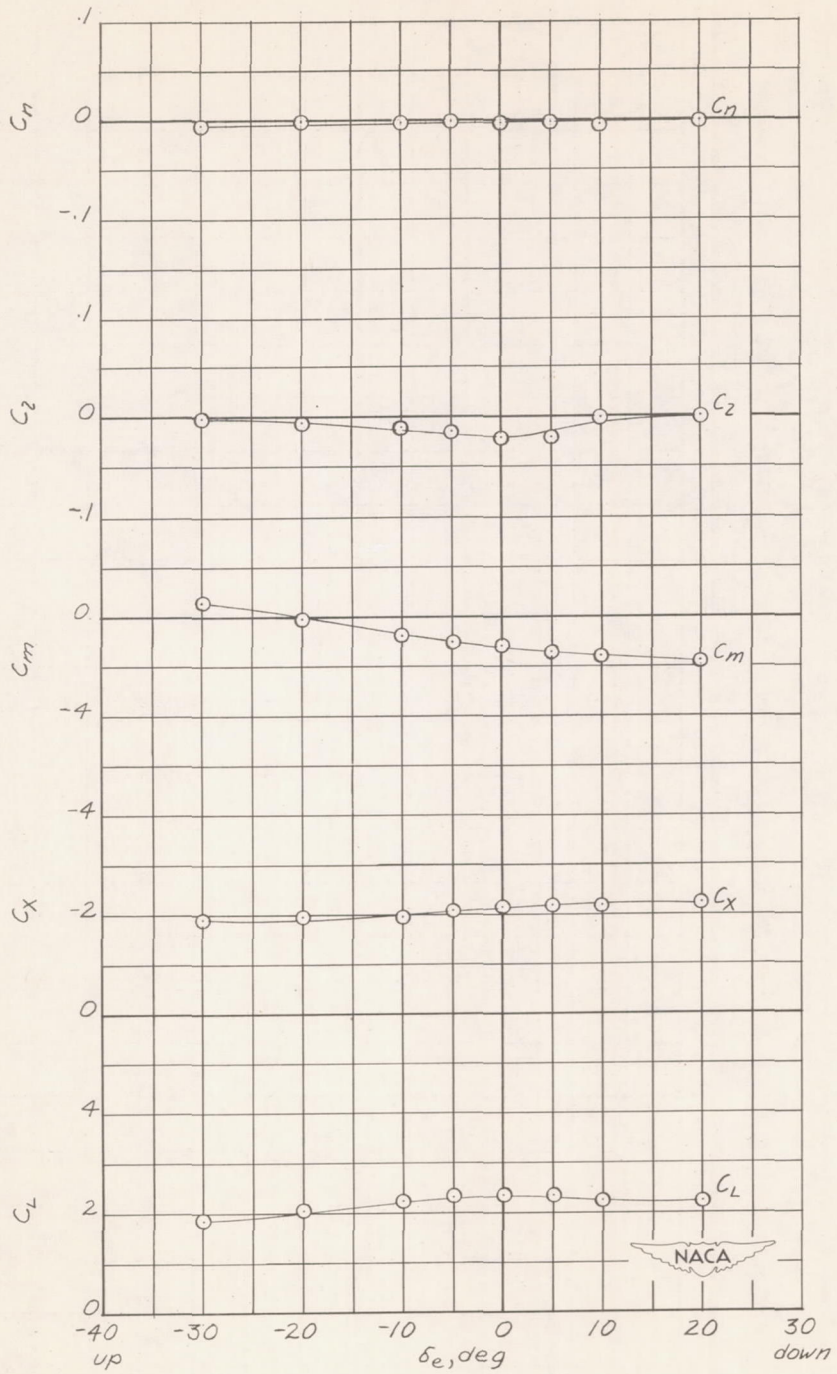

(a) $\delta_r = 0^\circ$; q = 1.70 lb/sq ft; ρ = 0.002324 slug/cu ft.

Figure 16.- Effect of control deflection on the aerodynamic characteristics of the Custer Channel Wing airplane. Propellers windmilling. $\alpha = 36^\circ$.

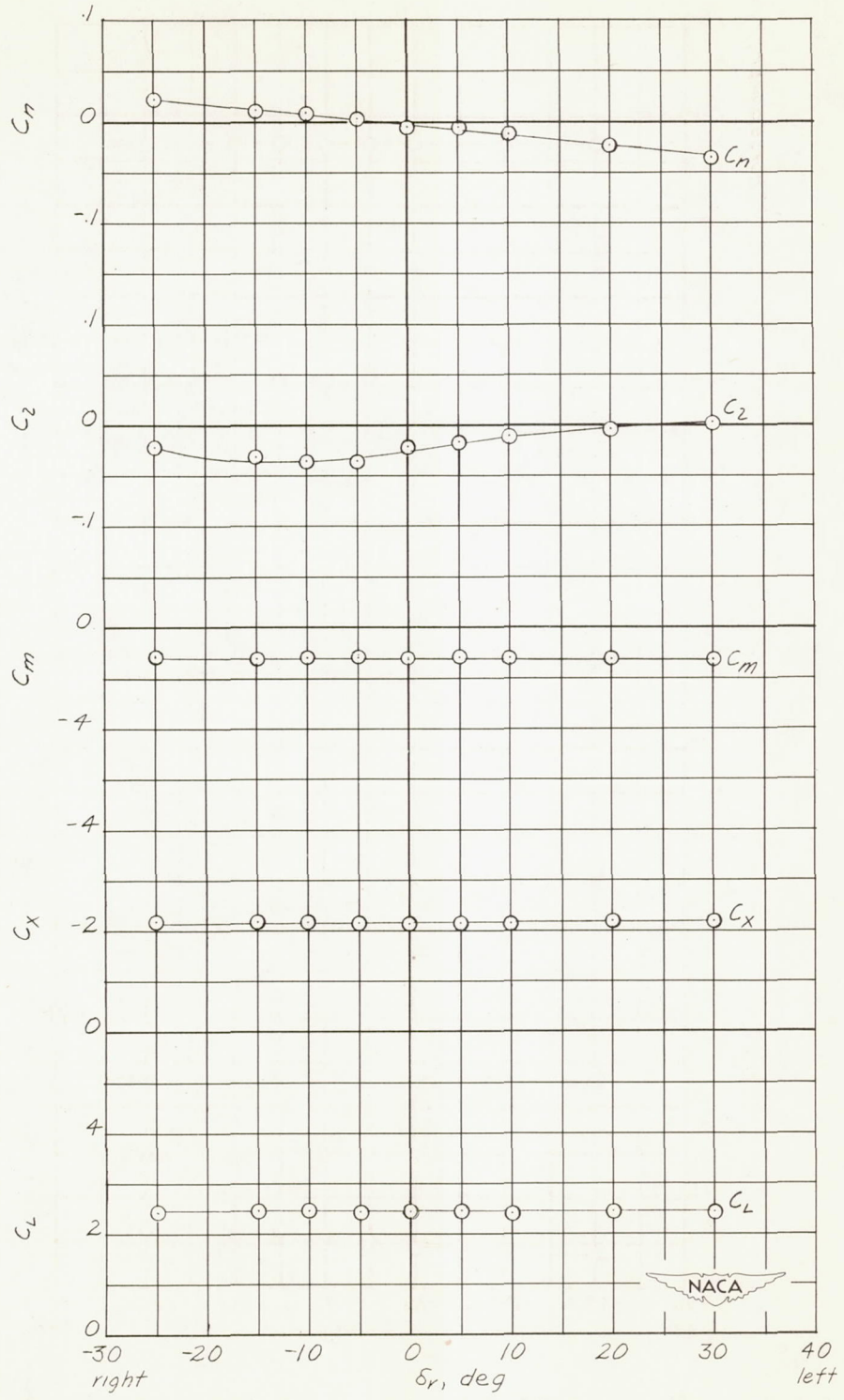

(b) $\delta_e = 0^\circ$; q = 1.74 lb/sq ft; ρ = 0.002323 slug/cu ft.

Figure 16.- Concluded.

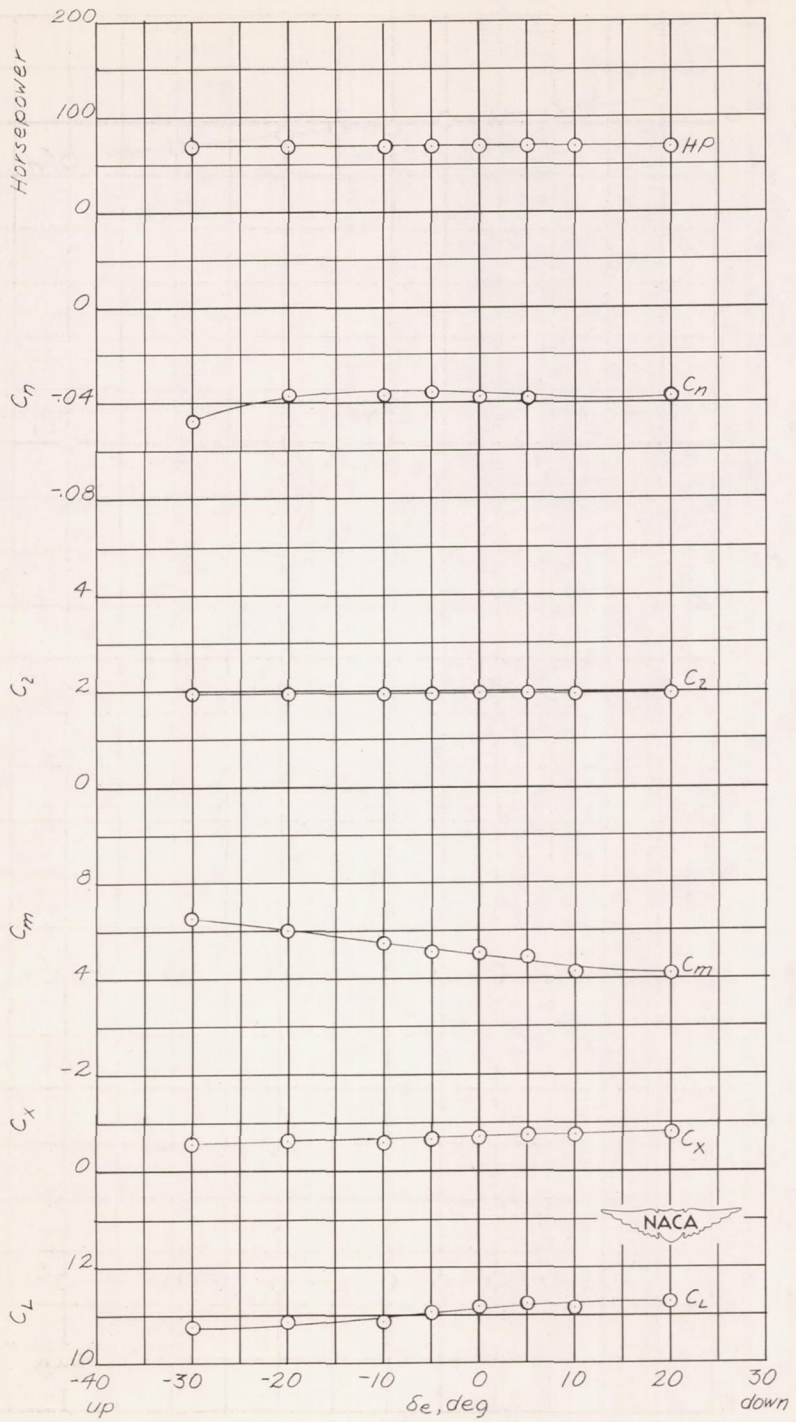

(a) $\delta_r = 0^\circ$; q = 1.78 lb/sq ft; ρ = 0.002330 slug/cu ft.

Figure 17.- Effect of control deflection on the aerodynamic characteristics of the Custer Channel Wing airplane with asymmetric power. Port propeller operating at 2,450 rpm. $\alpha = 33.8^\circ$.

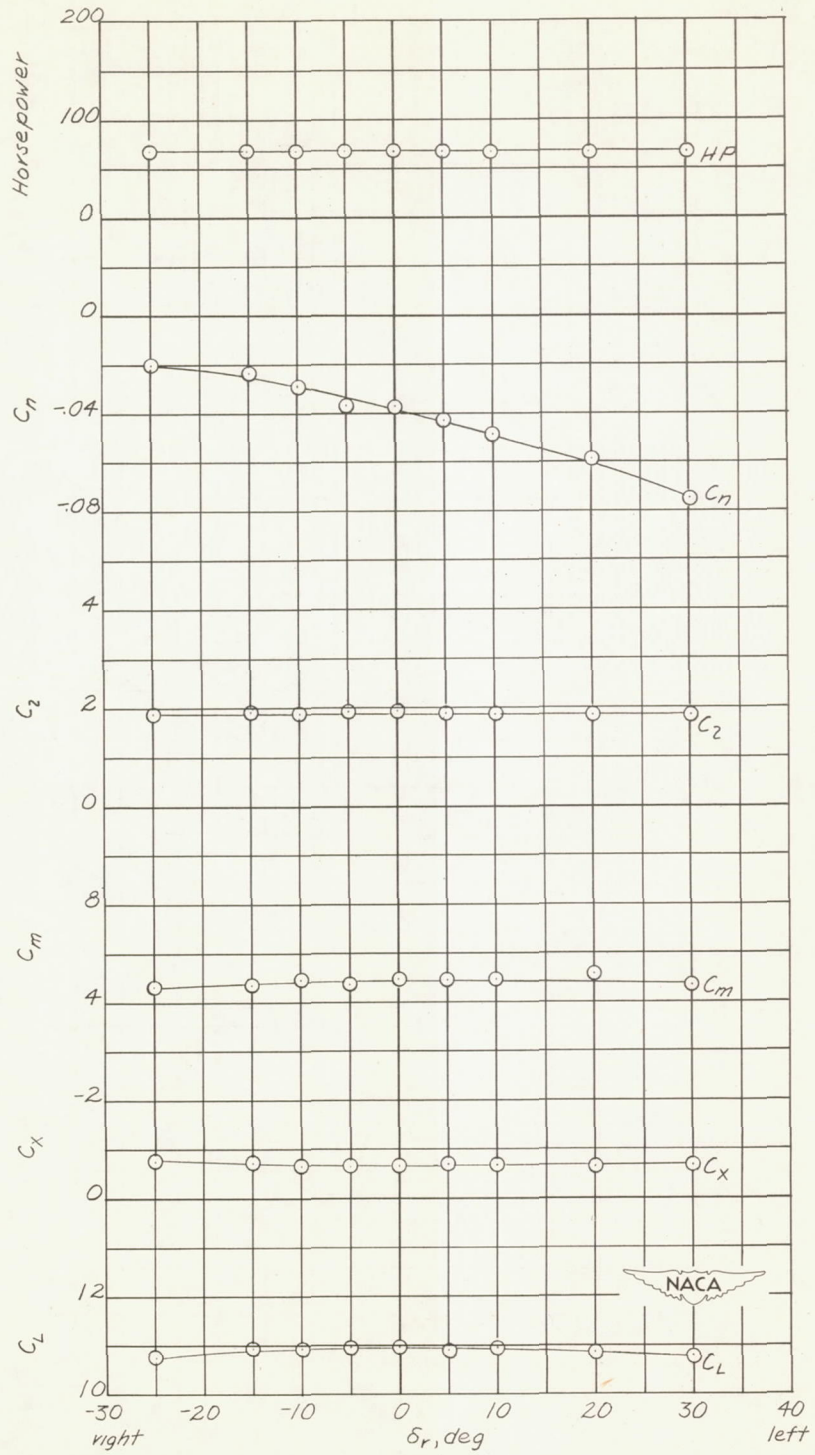

(b) $\delta_e = 0^\circ$; q = 1.78 lb/sq ft; ρ = 0.002330 slug/cu ft.

Figure 17.- Concluded.

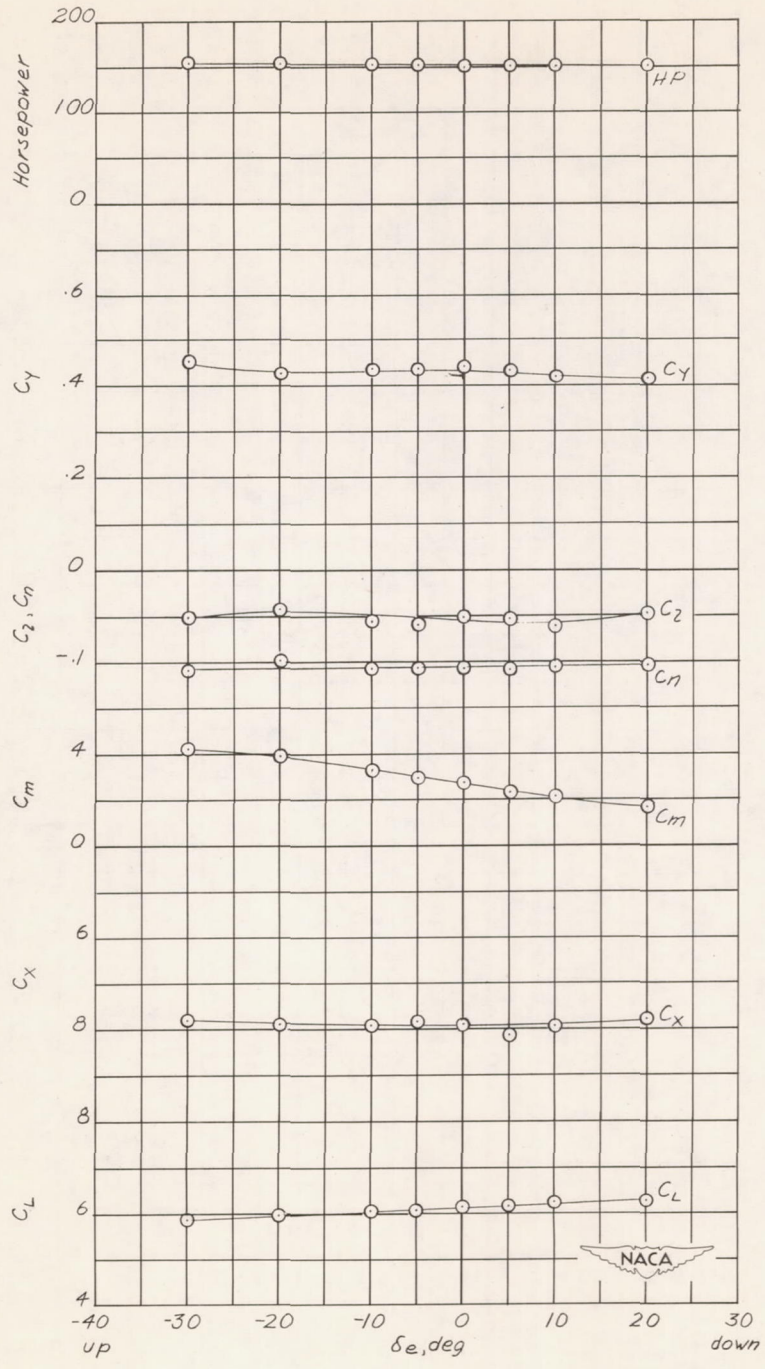

(a) $\beta = -5.06^\circ$; $\alpha = -2.0^\circ$; $\delta_r = 0^\circ$; $q = 2.20$ lb/sq ft; $\rho = 0.002330$ slug/cu ft.

Figure 18.- Effect of control deflection on the aerodynamic characteristics of the Custer Channel Wing airplane in sideslip. Propellers operating at 2,450 rpm.

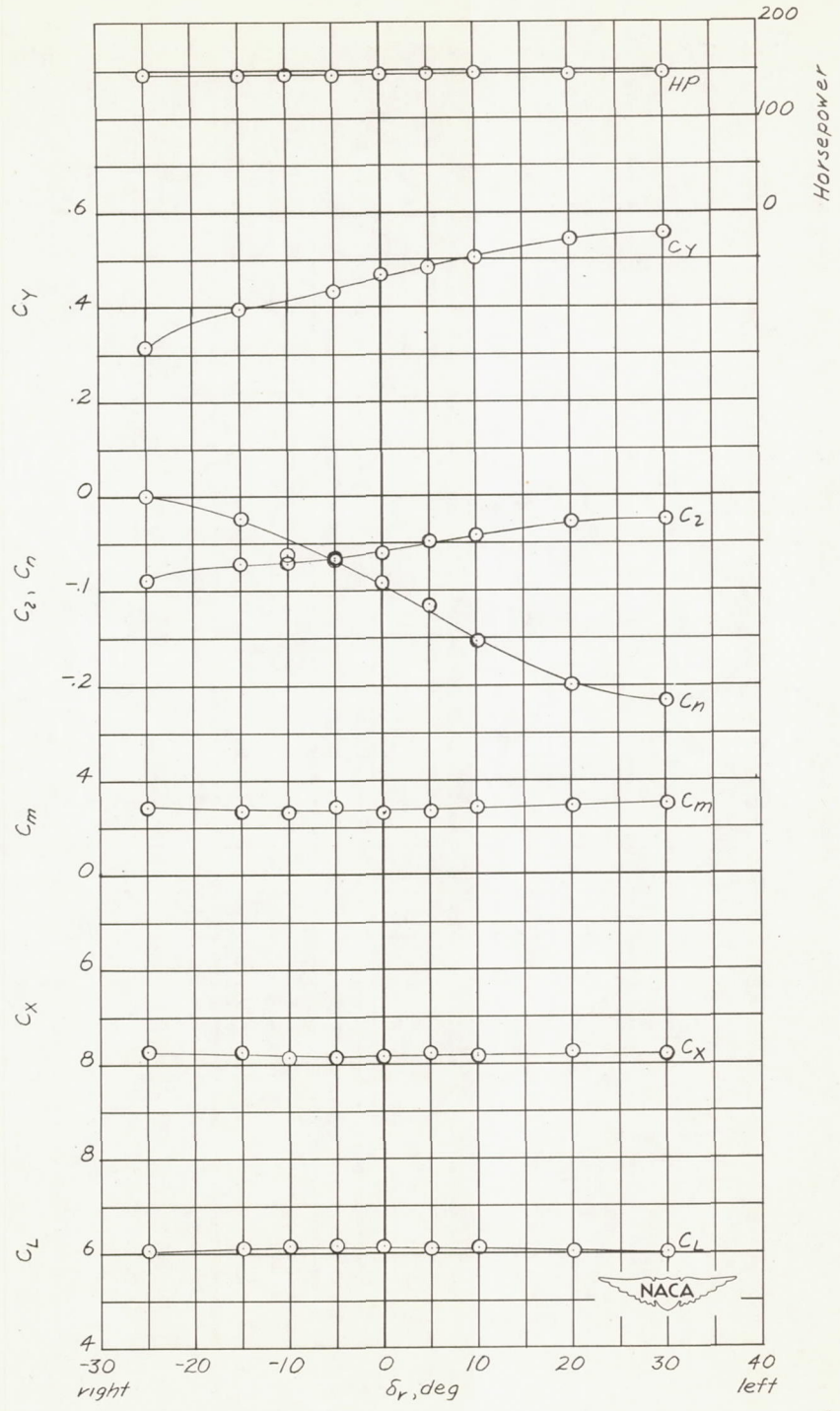

(b) $\beta = -5.06^\circ$; $\alpha = -2.0^\circ$; $\delta_e = 0^\circ$; $q = 2.19$ lb/sq ft; $\rho = 0.002346$ slug/cu ft.

Figure 18.- Continued.

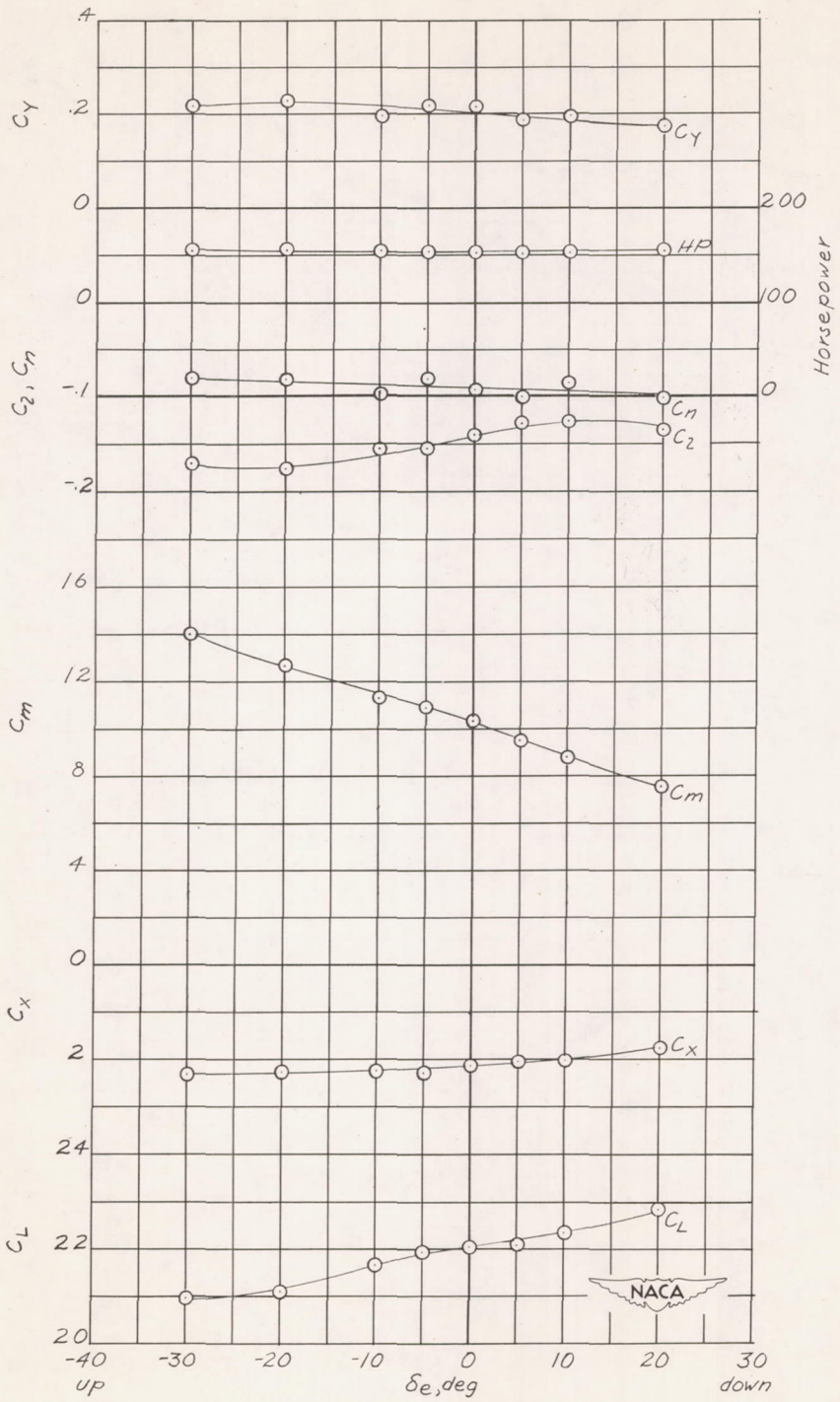

(c) $\beta = -5.06^\circ$; $\alpha = 31.1^\circ$; $\delta_r = 0^\circ$; $q = 1.71$ lb/sq ft; $\rho = 0.002317$ slug/cu ft.

Figure 18.- Continued.

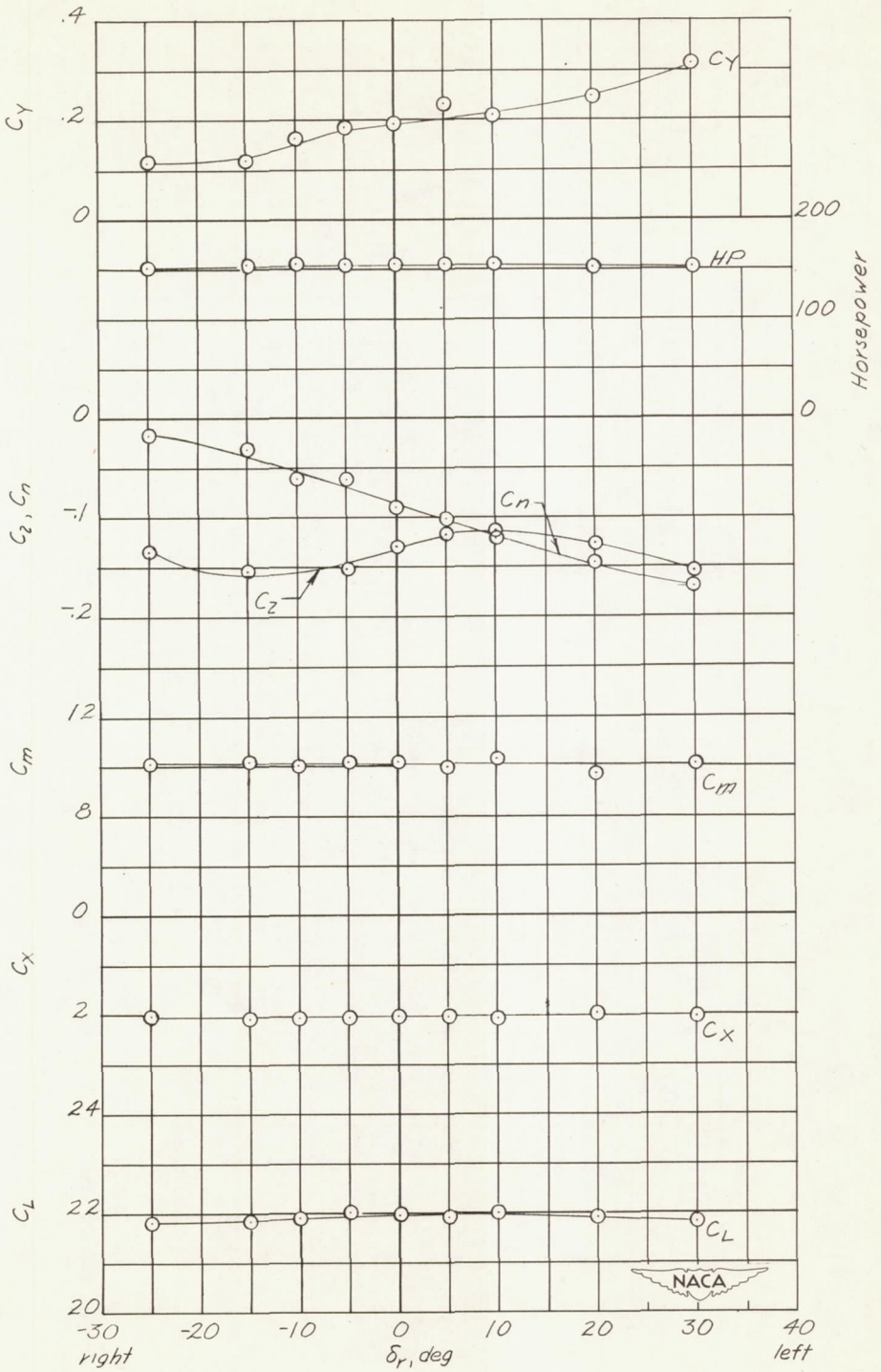

(d) $\beta = -5.06^\circ$; $\alpha = 31.1^\circ$; $\delta_e = 0^\circ$; $q = 1.71$ lb/sq ft; $\rho = 0.002315$ slug/cu ft.

Figure 18.- Continued.

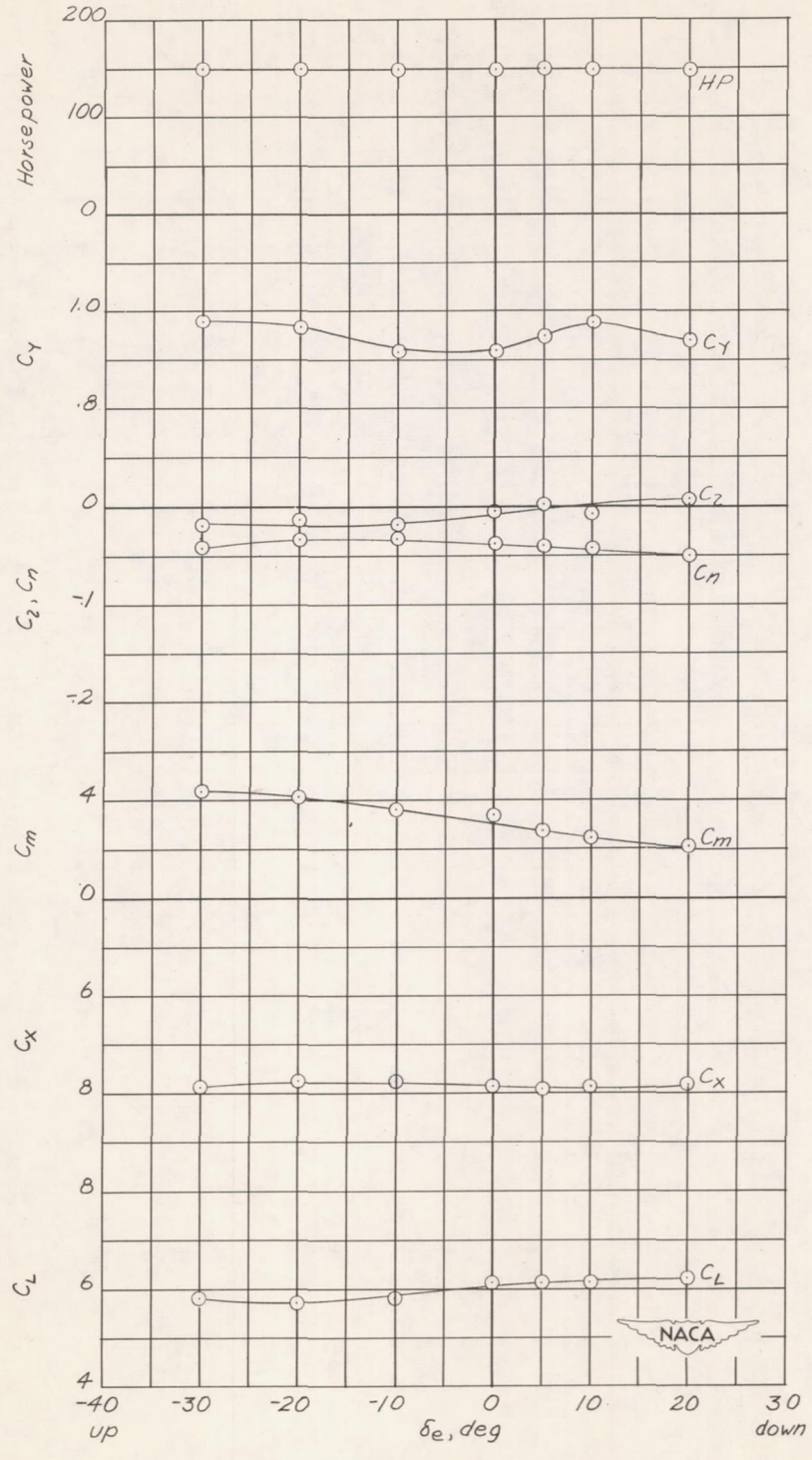

(e) $\beta = -9.83^\circ$; $\alpha = -2.0^\circ$; $\delta_r = 0^\circ$; $q = 2.20$ lb/sq ft; $\rho = 0.002320$ slug/cu ft.

Figure 18.- Continued.

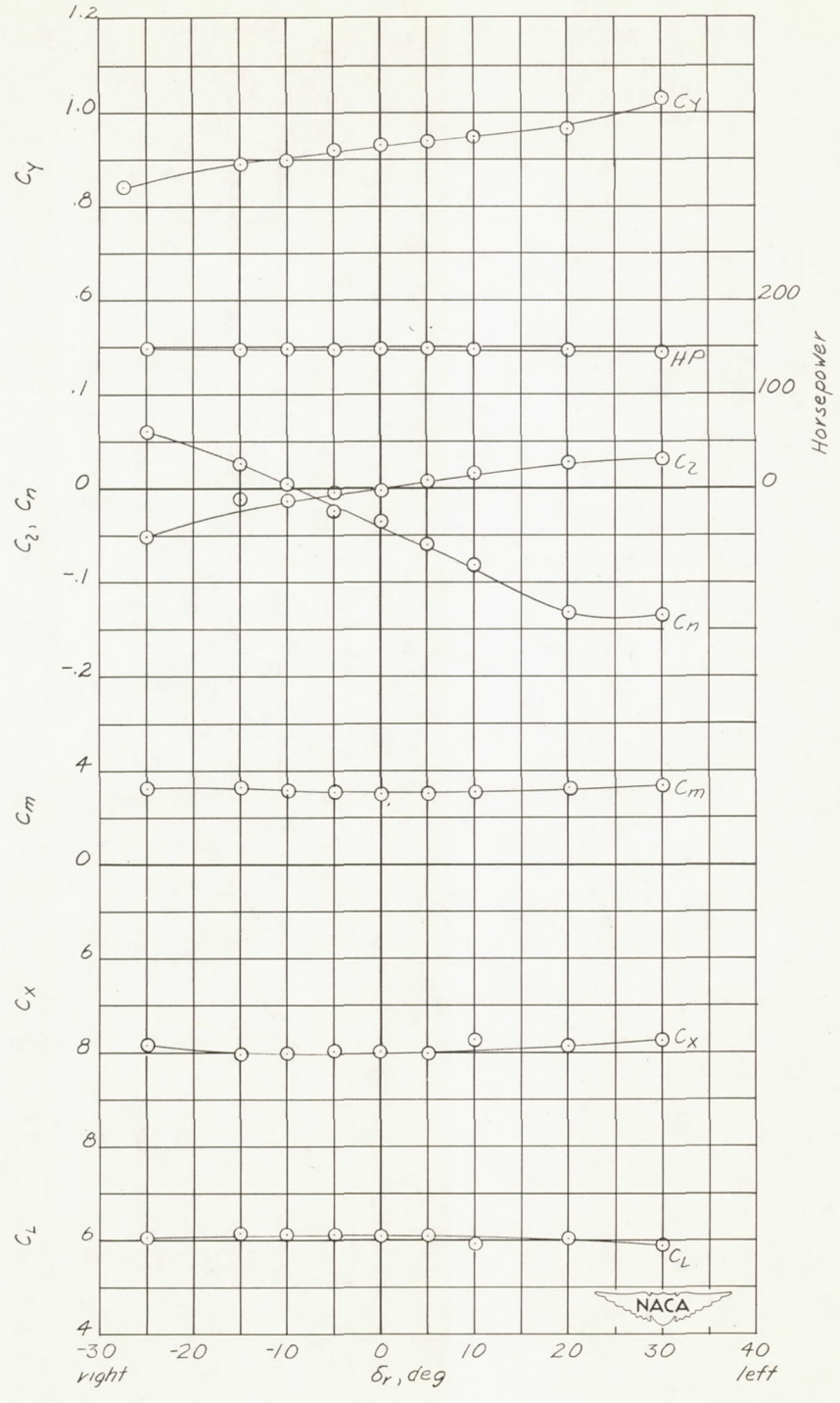

(f) $\beta = -9.83^\circ$; $\alpha = -2.0^\circ$; $\delta_e = 0^\circ$; $q = 2.17$ lb/sq ft; $\rho = 0.002324$ slug/cu ft.

Figure 18.- Continued.

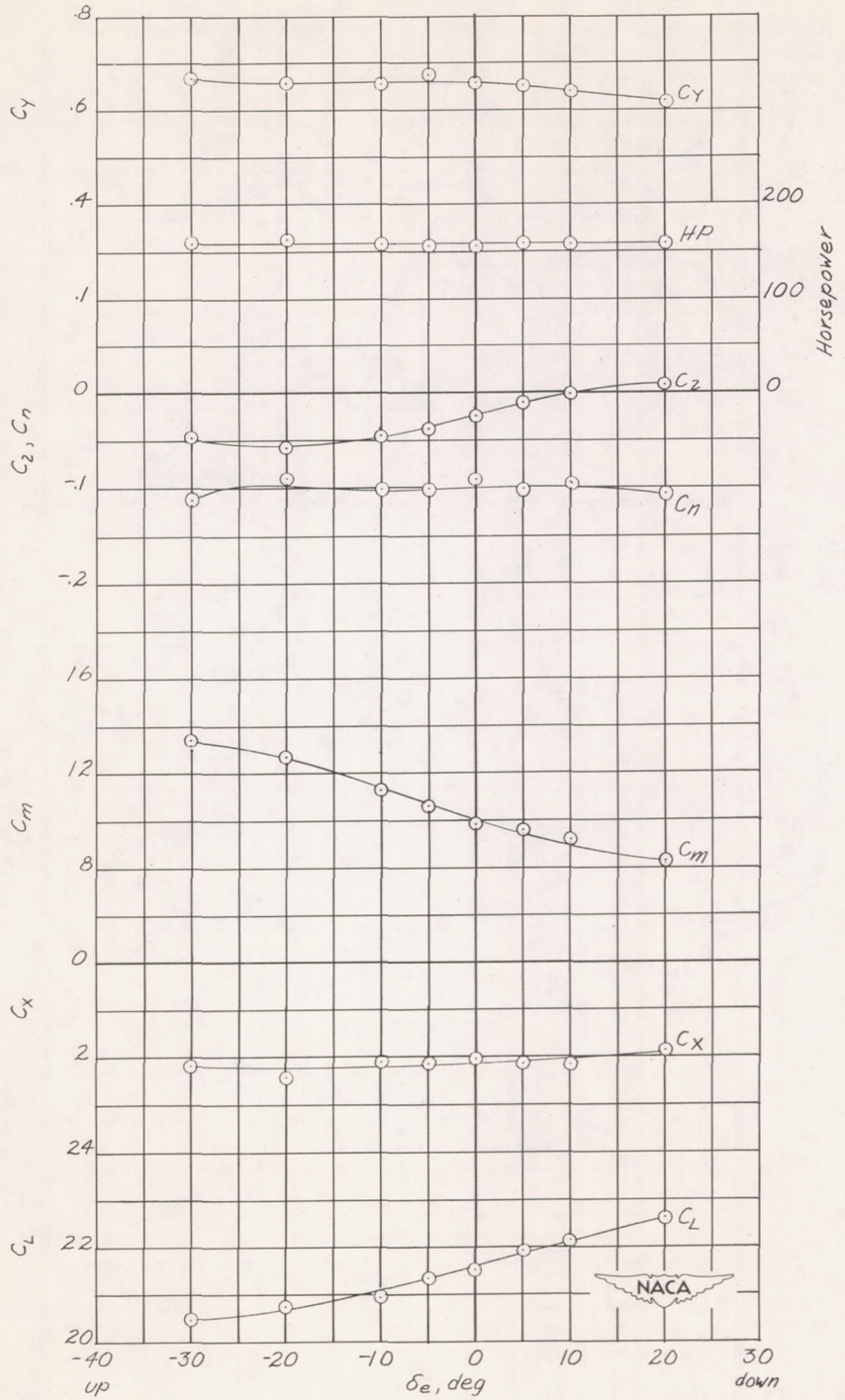

(g) $\beta = -9.83^\circ$; $\alpha = 31.1^\circ$; $\delta_r = 0^\circ$; $q = 1.73$ lb/sq ft; $\rho = 0.002337$ slug/cu ft.

Figure 18.- Continued.

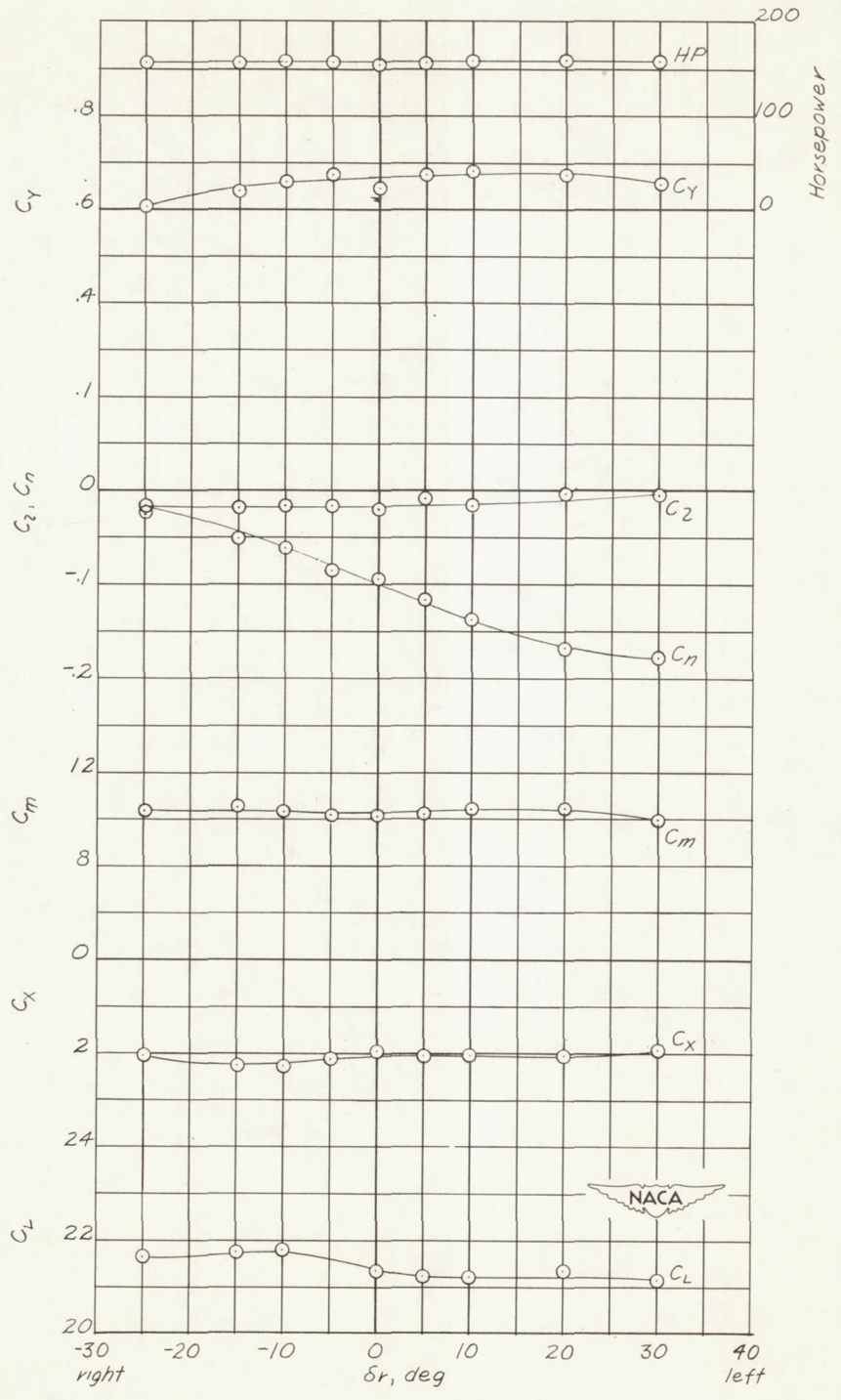

(h) $\beta = -9.83^\circ$; $\alpha = 31.1^\circ$; $\delta_e = 0^\circ$; $q = 1.74$ lb/sq ft; $\rho = 0.002337$ slug/cu ft.

Figure 18.- Concluded.

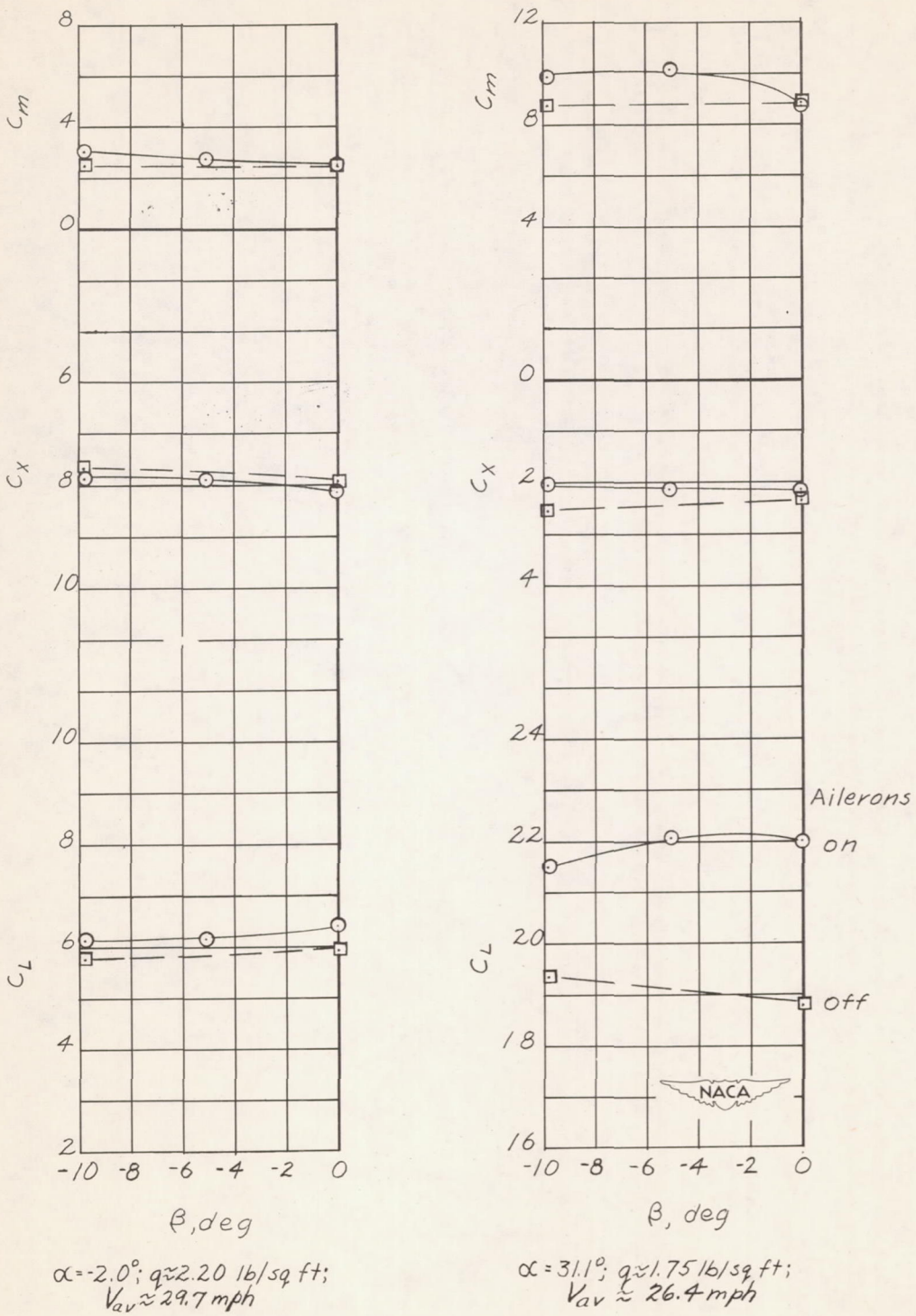

Figure 19.- Effect of ailerons on the longitudinal aerodynamic characteristics of the Custer Channel Wing airplane. Propellers operating at 2,450 rpm. $\delta_e = 0^\circ$; $\delta_r = 0^\circ$; aileron area, 17.5 sq ft.